NRC Publications Archive
Archives des publications du CNRC

Development of next generation hybrid batteries for zero-emission battery-electric locomotives
Neburchilov, V; Zhang, L.

NRC Publications Record / Notice d'Archives des publications de CNRC:
https://nrc-publications.canada.ca/eng/view/object/?id=fbddd4ff-62d9-46a4-a4ef-f7977b6324aa
https://publications-cnrc.canada.ca/fra/voir/objet/?id=fbddd4ff-62d9-46a4-a4ef-f7977b6324aa

National Research Council Canada   Conseil national de recherches Canada

Canada

NRC·CNRC **Energy, Mining and Environment**

Development of Next Generation Hybrid Batteries for Zero-Emission Battery-Electric Locomotives

Prepared for
Transportation Development Centre of
Transport Canada

by
National Research Council Canada

September 30, 2016

National Research
Council Canada

Conseil national de
recherches Canada

Canada

Development of Next Generation Hybrid Batteries for Zero-Emission Battery-Electric Locomotives

by
V. Neburchilov and L. Zhang,
National Research Council Canada

September 30, 2016

Disclaimer

This report reflects the views of the authors only and does not reflect the views or policies of NRC or the Transportation Development Centre of Transport Canada.

Neither NRC, Transport Canada, nor their employees, makes any warranty, express or implied, or assumes any legal liability or responsibility for the accuracy or completeness of any information contained in this report, or process described herein, and assumes no responsibility for anyone's use of the information. NRC and Transport Canada are not responsible for errors or omissions in this report and make no representations as to the accuracy or completeness of the information.

NRC and Transport Canada do not endorse products or companies. Reference in this report to any specific commercial products, process, or service by trade name, trademark, manufacturer, or otherwise, does not constitute or imply its endorsement, recommendation, or favoring by NRC or Transport Canada and shall not be used for advertising or service endorsement purposes. Trade or company names appear in this report only because they are essential to the objectives of the report.

References and hyperlinks to external web sites do not constitute endorsement by NRC or Transport Canada of the linked web sites, or the information, products or services contained therein. NRC and Transport Canada do not exercise any editorial control over the information you may find at these locations.

ABSTRACT

By 2020, transportation is expected to be the second largest source of greenhouse gas emissions; a trend that has been on the rise since 2005.

To reduce or eliminate emissions, replacing diesel locomotives with zero-emission battery-electric switcher locomotives for railroad applications must be considered a necessary option.

The potential use of a proposed hybrid battery, combining an asymmetric supercapacitor and lead-acid battery in battery-electric switcher locomotives, will allow the energy wasted during braking to be recovered and reused for locomotive acceleration.

The development of advanced electrodes of asymmetric supercapacitor and negative electrode lead-acid batteries and their optimal integration in a hybrid battery cell allows us to obtain its advanced performance.

The developed and fabricated hybrid battery (2V) cell prototype with a graded negative electrode demonstrates more than twice the capacity and a longer cycle life compared to conventional lead-acid batteries at high charge/discharge rates.

RÉSUMÉ

D'ici en 2020, le transport devrait être la deuxième source d'émissions de gaz à l'effet de serre, une tendance qui est en hausse depuis 2005.

Pour réduire ou éliminer les émissions, le remplacement des locomotives diesel par des locomotives électriques à commutation batterie-réseau s'impose comme l'option prioritaire pour des applications ferroviaires « à pollution zéro ».

L'utilisation de la batterie hybride proposée par nous, qui combine un supercondensateur asymétrique et une batterie au plomb, permettra aux locomotives électriques de récupérer l'énergie générée pendant le freinage et de la réutiliser pendant l'accélération.

Le développement des électrodes avancées pour le supercondensateur asymétrique et les électrodes négatives des batteries au plomb-acide, et leur intégration d'une manière optimisée dans la cellule de la batterie hybride, nous permet d'arriver à des performances avancées.

Le prototype de la pile hybride (2V) fabriqué, avec une électrode négative à gradient de concentration, a démontré plus de deux fois la capacité et une durée de vie plus longue à des taux de charge / décharge élevés, comparée aux batteries au plomb conventionnelles.

ACKNOWLEDGEMENTS

KEY WORDS:

- absorbed glass mat lead-acid battery

- asymmetric supercapacitor (ASC)

- battery-electric locomotives

- capacity

- cycle life

- high-rate partial-state-of-charge

- hybrid battery

- negative split electrode

- positive electrode

- valve regulated lead-acid battery

EXECUTIVE SUMMARY

The objective of this project is to develop a 2V hybrid battery cell, which combines an absorbed glass mat lead-acid battery cell and an asymmetric supercapacitor. This hybrid battery utilizes a novel negative electrode structure that provides no less than twice the capacity and has: a more durable structure, a longer cycle life, and better stability at higher charge/discharge rates than conventional lead-acid batteries.

An extensive literature and patent search, as well as an analysis of state-of-the-art hybrid batteries, asymmetric supercapacitors, and absorbed glass mat lead-acid batteries enabled the selection of the optimum direction of research and development of components for hybrid batteries, methods of their fabrication, integration into a cell prototype, and the development and utilization of test protocols.

The improved performance of the hybrid battery is based on buffer properties of its asymmetric supercapacitor and higher durability of the developed graded negative electrode. In contrast to hybrid battery negative electrode prototypes, the developed graded negative electrode has a more durable structure based on the graded carbon concentration (high carbon concentration of 1.2% on the surface and low carbon content of 0.7% in the bulk) assembled with a carbon electrode of the asymmetric supercapacitor.

The life cycle cost reduction of a hybrid battery cell compared to a lead-acid battery cell is based on its longer cycle life. The baseline of an asymmetric supercapacitor + absorbed glass mat lead-acid battery and their components was developed and fabricated. An optimized method for the integration of components in the hybrid battery has been tested and applied to the fabrication of a hybrid battery cell prototype.

The identification of the optimized high carbon content (1.2%) in graded negative electrode and the selection of best components (specific types of carbon black for hybrid battery, graded negative electrode and asymmetric supercapacitor) allowed us to address the negative electrode sulfation problem efficiently.

Hybrid batteries with optimized graded negative electrode allow for extended applications of advanced lead-acid batteries which would, for example, improve their performance in battery-electric locomotives. This advanced hybrid battery (2V) cell prototype has been developed, fabricated, and successfully tested, and these achievements have created opportunities for further development of more powerful hybrid batteries (12V).

SOMMAIRE

L'objectif du projet est le développement d'une cellule hydride de 2V qui combine une cellule plomb-acide sulfurique (lead-acid battery, LAB) á séparateurs en fibre de verre absorbante (Absorbed Glass Mat, AGM) et un supercondensateur asymétrique (asymmetric supercapacitor, ASC). La cellule utilise une nouvelle structure de l'électrode négative et fournit plus que deux fois la capacité, a une durée de vie plus longue et une meilleure stabilité aux taux de charge / décharge élevés que les accumulateurs au plomb classiques.

Une recherche approfondie de la littérature et des brevets, suivie par une analyse du développement des technologies liées aux batteries hybrides, aux condensateurs asymétriques et aux batteries au plomb á séparateurs en fibre de verre absorbante, ont permis de sélectionner la direction de la recherche et du développement de composants pour batteries hybrides

La performance améliorée de la batterie hydride proposée dans ce projet est le résultat des propriétés de tampon de son supercondensateur asymétrique et à une durabilité plus élevée de l'électrode négative á gradient (graded negative electrode, GNE). Contrairement aux prototypes d'électrode négative pour les batteries hybrides, la GNE proposée a une structure plus durable, basée sur la combinaison entre le gradient de la concentration de carbone (teneur élevée en carbone de 1,2% en surface et faible teneur en carbone de 0,7% dans la masse) et l'électrode de carbone du supercondensateur asymétrique.

La réduction des coûts associes au cycle de vie de la cellule hybride par rapport à la cellule LAB est basée sur sa durée de vie plus longue. Les composants de la version de référence de la combinaison cellule plomb-acide sulfurique á séparateurs en fibre de verre absorbante+supercondensateur asymétrique ont été développés et fabriqués. Une méthode optimisée d'intégration des composants dans la batterie hybride a été testée et appliquée à la fabrication d'un prototype de la cellule.

L'identification de la teneur optimale en carbone (1,2%) dans l'électrode négative á gradient et la sélection des meilleurs composants (types spécifiques de noir de carbone pour la batterie hybride, l'électrode négative á gradient, et le supercondensateur asymétrique) nous ont permis de résoudre d'une manière efficace le problème de la sulfatation de l'électrode négative.

Les batteries hybrides avec une électrode négative á gradient optimisé permettent l'utilisation des batteries au plomb (LAB) dans des applications avancées, comme, par exemple, des batteries pour les locomotives à batterie électrique (BEL). La cellule bybride avancée (2V) a été développée, fabriquée et testée avec succès. Ces réalisations ont mis la base pour le développement des batteries hybrides encore plus puissantes (12V).

Contents

LIST OF FIGURES

LIST OF TABLES

LIST OF ACRONYMS

ASC	Asymmetric Supercapacitor
BEL	Battery-Electric Locomotive
CSIRO	Commonwealth Scientific and Industrial Research Organisation (Australia)
CV	Cyclic Voltammogram AGM VRLAB
C	Capacity
CAGR	Compound Annual Growth Rate
EDLC	Energy Density of an Asymmetric
GHG	Greenhouse Gas
HB	Hybrid Battery
HEV	Hybrid Electric Vehicles
HRPSoC	High Rate Partial State-of-Charge
LAB	Lead-Acid Battery
LIC	Lithium-ion Capacitor
LiB	Lithium-ion Battery
NAM	Negative Active Material
NE	Negative Electrode
NiMH	Nickel Metal Hybrid Battery
PE	Positive Electrode
PbC	Asymmetrical super Capacitive Lead-Acid Hybrid Battery of the Company 'Axion'

1 INTRODUCTION

By 2020, transportation is expected to be the second largest source of greenhouse gas emissions; a trend that has been on the rise since 2005. In 2009, the Government of Canada committed to reducing its greenhouse gas emissions to 607 Megatonnes (Mt) or 17% below the 2005 levels by 2020[1], and Transport Canada is working on a number of fronts to help with this reduction. One such effort involves managing science and technology projects to develop a transportation system with significantly reduced emissions. The Clean Transportation Initiative (CTI) was developed in response to this commitment: to reduce transportation related emissions through regulations, support the adoption of clean technologies and practices, and engage in research technologies and practices.

Locomotives are a large contributing factor of greenhouse gas emissions, therefore, to reduce or eliminate these emissions, replacing diesel locomotives with zero-emission battery-electric switcher locomotives for railroad applications must be considered a necessary option. The two main challenges however in the development of battery-electric switcher locomotives are the high costs associated, and insufficient cycle life. Thus this project will address the technical and economic gaps in the development of cost-effective and high performance batteries such as hybrid batteries for locomotive applications.

The potential use of hybrid batteries in battery-electric switcher locomotives would allow the energy wasted during braking to be recovered and reused for locomotive acceleration, which would increase gas efficiency and decrease air emissions. Hybrid batteries combine an asymmetric supercapacitor and an advanced absorption glass mat lead-acid battery, which allows the coupled asymmetric supercapacitor to significantly improve both the power and cycle life of hybrid batteries as it acts as a buffer during high-rate partial state-of-charge. Therefore, hybrid batteries can transfer and accumulate a charge very quickly during the battery-electric switcher locomotives acceleration and regenerative braking process. Although absorption glass mat lead-acid batteries have a low cost, their running costs are high due to a short cycle life.

Hybrid batteries with a split negative electrode have many advantages, including: (1) longer cycle life, (2) faster charging at high-rate partial state-of-charge, (3) simple thermal management, (4) higher cost-efficiency, and (5) no safety issues. Consequently, the project objective is to develop a hybrid battery (2V) with an advanced negative electrode to achieve longer cycle life at high-rate partial state-of-charge and cost reduction in comparison with advanced lead-acid batteries.

2 LITERATURE REVIEW

2.1 Asymmetric Supercapacitors (ASC)

Supercapacitors (SCs) are one of the most promising energy storage devices so far developed due to their high power density, high efficiency, short recharging time, and long shelf and cycle life. They are particularly well-suited for electric and hybrid vehicles, for which they can provide acceleration power and braking energy recovery. Combining supercapacitors and batteries can significantly improve battery lifetime and the energy recovery efficiency in braking in electric vehicle applications in which the vehicle power sources are subject to high current pulses in both the charge and discharge.[2]

Supercapacitors are relatively new systems for energy storage. While small SCs (a few farad cells) have been used in electronic devices since the mid-1990s, their implementation in the Airbus A380 jumbo-jet for emergency door opening has placed SCs as the most reliable energy storage devices.[3]

Their characteristics differ significantly from those of other known energy storage devices, such as batteries (Li-ion, Lead-acid, NiMH, NiCd,) or dielectric capacitors. Their use will rarely replace but will rather complement these devices, according to the energy and power requirement of the specific application[4]. The energy storage and release characteristics of SCs can be represented by the Ragone plot of Figure 1.[5] This graphic represents the energy vs. the power of the system. Capacitors (in grey on the graphic) store energy as surface charges on dielectric plates. No chemical reactions are involved in this process, and it ensures a very fast release of energy; that is, power. However, they can only store charges at the surface of their flat electrodes, and are therefore unable to store very much energy. They are used for applications which require a quick release of energy, and are typically discharged below the millisecond range.[6]

On the other hand, rechargeable batteries (in green on the graphic) store energy by electrochemical reactions that use the bulk of the materials. They can consequently store large amounts of energy (depending on the specific chemistry of the battery). Their power (speed of energy release) is limited by the kinetics of the chemical reactions involved, which usually prevents them from having high power capabilities. They are used for applications that do not need much power, but require long times of charge and discharge, from minutes to hours.[11]

For quite some time, there was a gap between these two categories of charge storage devices: storage and release of energy in the time range of 0.1 to 100s. This gap is now filled by SCs (in blue in the graphic) as these systems are able to release more energy than capacitors but less than batteries. On the other hand, they have more power than batteries but less than capacitors.[7,6] A great advantage of SCs versus batteries is their safety and cyclability: while batteries typically last for a few thousand charge/discharge cycles due to the deterioration of active materials during cycling, SCs can be used for millions of cycles, as they only involve electrostatic charge storage, as in the case of dielectric capacitors.
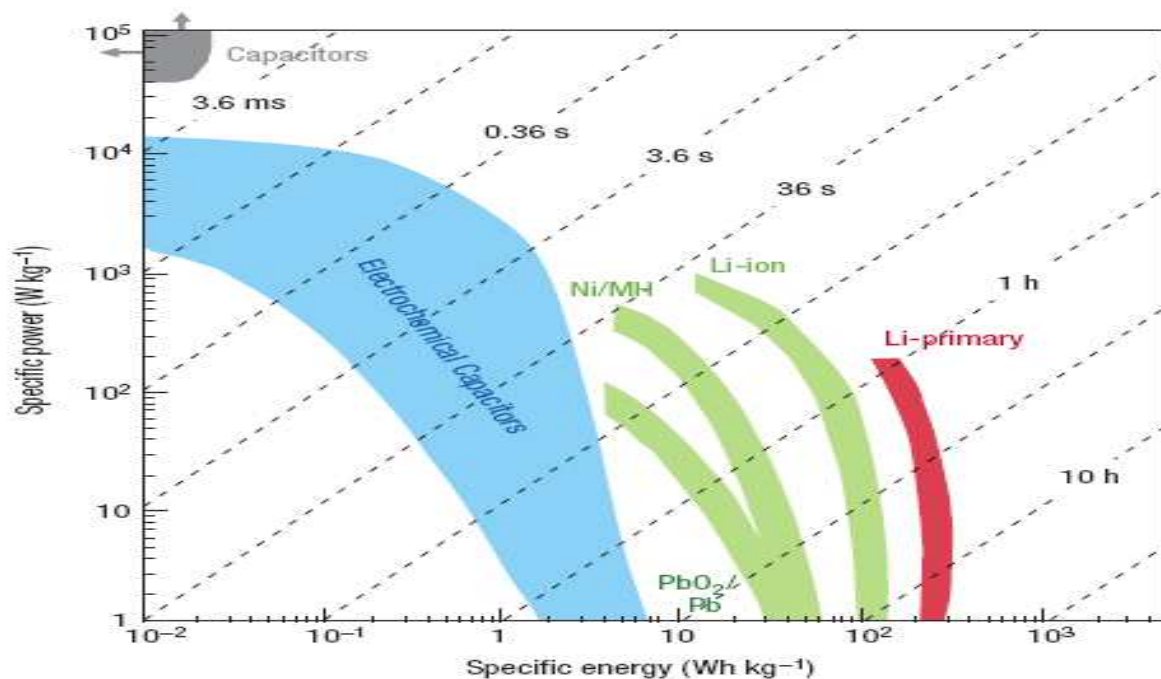
Figure 1: Ragone plot of various energy storage devices. The time indicated corresponds to the time constant of the cells.[5]

Recent years have yielded major progress in the theoretical and practical research and development of SCs, as evinced by a large number of research articles and technical reports.[6-14] The supercapacitor term includes three kinds of systems, which have different active materials but share a number of characteristics: carbon-based SCs (or electrochemical double-layer capacitors: EDLCs), metal oxide SCs, and conducting polymer SCs.[8-10]

2.1.1 Electrochemical Double Layer Supercapacitors (EDLCs)

The name supercapacitor comes from these devices: they store energy as surface charges (like capacitors) but their electrodes are composed of carbon powders developing very high

surface areas (typically over 1000 m^2/g)[10]. Using carbon as the active material, EDLCs today represent more than 80% of commercially manufactured SCs. Their energy is stored at the

electrolyte/carbon interface by charging the "double-layer capacitance" through reversible ion adsorption on the carbon surface. No redox reaction is thus involved in the charge storage mechanism of EDLCs.

The active material used in EDLCs is carbon, since it offers a combination of electrical conductivity, high specific surface area (SSA), and electrochemical stability over a wide range of potentials in both aqueous and non-aqueous electrolytes.[11] Since energy is directly linked to surface area, they can store significantly more energy than capacitors. However, double-layer capacitors store charges in the form of ions, and the speed of this process is limited by the diffusion kinetics of these ions at the surface of the electrodes, which gives them less power than dielectric capacitors.

On the other hand, in spite of these large specific surface areas of carbon particles, the charges physically stored on the carbon particles in porous electrode layers are unfortunately limited. These kinds of electrochemical double-layer supercapacitors have a limited specific capacitance (measured in Faradays per gram of the electrode material) and a low SC energy density.

Figure 2 shows a typical double-layer SC cell.[6] The device contains two carbon electrodes (schematized as flat plates for the clarity of the figure, but which are composed of finely spread carbon powders) deposited on current collectors (typically metallic plates or grids) and separated by an electrolyte (ions + liquid or polymer gel). To prevent short-circuits, a porous separator is placed between the electrodes. In a real cell, the stack composed of the two electrodes and the separator are pressed together and soaked in the electrolyte. This can later be aqueous (generally a strong acid or a strong base) or an organic solvent (acetonitrile, carbonates).
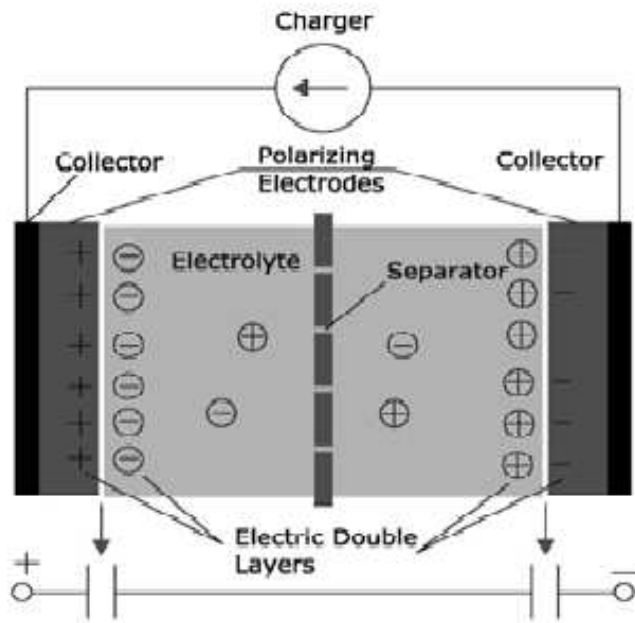
Figure 2: Schematic cell of a carbon double-layer supercapacitor.[6]

2.1.2 Faradaic Supercapacitors (FS)

Faradaic supercapacitors (FS), or pseudocapacitors, are different from electrostatic or EDLCs. When an electric potential is applied to an FS, fast and reversible faradaic reactions (redox reactions) take place on the electrode materials and involve the passage of charge across the double layer; similar to the charging and discharging processes that occur in batteries, resulting in faradaic current's passing through the supercapacitor cell. Materials undergoing such redox reactions include conducting polymers and several metal oxides, including RuO_2, MnO_2, and Co_3O_4.[12-16] Three types of faradaic processes occur at FS electrodes: reversible adsorption (for example, adsorption of hydrogen on the surface of platinum or gold), redox reactions of transition metal oxides (i.e.: RuO_2), and reversible electrochemical doping–de-doping in conductive polymer-based electrodes.[13]

It has been demonstrated that these faradaic electrochemical processes not only extend the working voltage but also increase the specific capacitance of the supercapacitors.[17] Since the electrochemical processes occur both on the surface and in the bulk near the surface of the solid electrode, an FS exhibits far larger capacitance values and energy density than an EDLC. As reported by Conway et al.[18] the capacitance of a FS can be 10–100 times higher than the electrostatic capacitance of an EDLC. However, a FS usually suffers from lower power density than EDLC because faradaic processes are normally slower than non-faradaic processes.[18] Moreover, because redox reactions occur at the electrode, a FS often lacks stability during cycling, similar to batteries.

Regarding advanced SC materials, metal oxides such as ruthenium oxides and manganese oxides are considered the most promising materials for the next generation of SCs. Metal-oxide supercapacitors (RuO_2, IrO_2) use protonation of the oxides in acidic conditions.[6] Metal oxide SCs store the most energy but suffer from very high costs due to the rare metals they use. They are therefore limited to defense or space applications. Recent developments on cheap MnO_2 materials could pave the way to promising systems, even if MnO_2 has much lower capacitance properties than RuO_2 or IrO_2 systems. Moreover, MnO_2 can be used in mild electrolytes, rather than strong acids or bases, which has an obvious advantage in terms of safety.

Conducting polymer supercapacitors use the doping/undoping phenomenon of these very particular polymers to store charges in the form of ions (like double-layer capacitors).[19,20] However, all the bulk of the polymer participates in the storage activity, not just the surface layer. This characteristic allows these systems to charge more energy than carbon double-layer capacitors. These systems are still at the development stage and still suffer from progressive degradation of the active materials with cycling.

Radical polymer supercapacitors are the more recently discovered class of pseudo-capacitive materials.[23,24] They store/release energy through doping/undoping processes as conducting polymers. These materials are still at the development stage for their use in supercapacitors and lithium-ion batteries.

EDLCs with both electrodes made of identical materials are called symmetric. EDLCs with electrodes of different compositions are called asymmetric. In asymmetric EDLCs (also

known as hybrid supercapacitors) typically one electrode is based on carbon, representing the capacitive element, while the other can be a metal oxide (pseudocapacitive element) or a conductive polymer. Asymmetric EDLCs (or AEDLCs) allow for higher energy density devices due to various factors.

It is worth mentioning that hybrid supercapacitors with an asymmetrical electrode configuration (i.e.: one electrode consists of electrostatic carbon material while the other consists of faradaic capacitance material) have been extensively studied of late to capitalize on both electrode materials' advantages in improving overall cell voltage and energy, and power densities.[25,26] In this kind of hybrid supercapacitor, both electrical double-layer capacitance and faradaic capacitance mechanisms occur simultaneously, but one of them plays a greater role. In a capacitor the following relationship always holds:

$1/C = 1/C1 + 1/C2$

In this equation, C = device capacitance, C1 = specific capacitance of the first electrode, and C2 = specific capacitance of the second electrode.

For example, if the electrodes were the same (both carbon) with specific capacitance equal to 1 F, the device capacitance would be equal to 0.5 F; whereas, if C1 (metal oxide) = 2 F and C2 (carbon) = 1 F, C would be equal to 0.7 F (i.e., closer to the carbon type). The mere fact of using an asymmetric design results in a higher capacitance (in the above example, 0.7 F versus 0.5 F) than a symmetric design with low capacitance electrodes. Thus, the asymmetric design inherently allows for a higher energy density. In addition, since the capacitance of the device is largely determined by the electrode with the smallest specific capacitance, the electrode (metal oxide) with higher capacitance can be built with smaller dimensions compared to the carbon electrode, thus reducing the device weight (which increases the energy density).

Thanks to its water oxidation overpotential, the use of faradaic capacitance materials, such as metal oxide, enables an increase in water's electrochemical stability. As the supercapacitor energy storage capacity is proportional to the square of the voltage, this voltage increase is a tremendous opportunity to increase the supercapacitor's performances. The combination of these three factors has been found to increase the energy density of an asymmetric EDLC by a factor of 8 compared with symmetric supercapacitors.

New research tendencies in supercapacitors include the development of hybrid devices, which try to get the best from each system by combining them.[28] Supercapacitor/battery hybrid devices[29,30] include lithium ion capacitors and hybrid batteries. A lithium ion capacitor (LIC) consists of a positive electrode made of activated carbon material, a negative electrode made of carbon material doped with lithium ions, and a lithium-based electrolyte. LICs are characterized by high cell voltages of up to 4 V.

A hybrid battery is a device in which a lead-acid battery and an asymmetric supercapacitor are embedded in the same cell. These systems share the positive electrode, while the negative electrodes of the battery and the supercapacitors can be connected in parallel. Hybrid devices have electrical properties that are between those of EDLCs and batteries, and they exhibit improved lifetime and input/output characteristics over standard batteries. In

addition, when compared to separate batteries and supercapacitors connected together, they are more economical, occupy less space, and do not require an electronic control circuit.

Another of the new promising research avenues is the use of nanostructured active materials, which leads to significant power enhancement by allowing quick access of the electrolyte ions to the surface of the active material.[5, 31, 32]

Supercapacitors are being manufactured and marketed by a number of companies around the world. According to a recent Frost & Sullivan report, their total market revenue was $267.6 million in 2013, and it is expected to experience a compound annual growth rate (CAGR) of 12.2% from 2013 to 2020.[33] SCs are used in three main markets: consumer electronics, industry, and transportation.[34] This last market is foreseen to take the lead quickly due to the rapid development of electric and hybrid vehicles.[35,36] Specifically in vehicles, SCs are used or envisioned for: 1) stop-and-go applications; 2) regenerative braking; 3) peak power supply during vehicle acceleration (complementary to the battery or fuel cell); and 4) electronics powering. Moreover, more and more small markets for SCs are being continuously identified, particularly in consumer electronics, as end-users are discovering this new category of energy storage devices.

2.2 Advanced Lead-Acid Batteries

2.2.1 Absorbed Glass Mat Valve-Regulated Lead-Acid Batteries (AGM VRLAB)

Recently, traditional lead-acid batteries (LAB) were significantly modified with the partial and full replacement of lead-based negative active material (NAM) with carbon that allowed for a significant increase in the battery cycle life and reduction of its cost and weight. The conventional lead acid battery consists mainly of the negative lead electrode, positive lead oxide electrode, separator, and electrolyte (sulfuric acid). During discharge, both electrodes are converted to lead sulfate, and the opposite process occurs during the battery's charge. The advanced lead-acid battery has a bipolar design (Fig.3), where the negative plate of one cell becomes the positive plate of the next cell. Cells are separated from each other by these bipolar plates, which enable the separate work of single cells and transmission of positive electrode potential to the negative plate.

a) b)
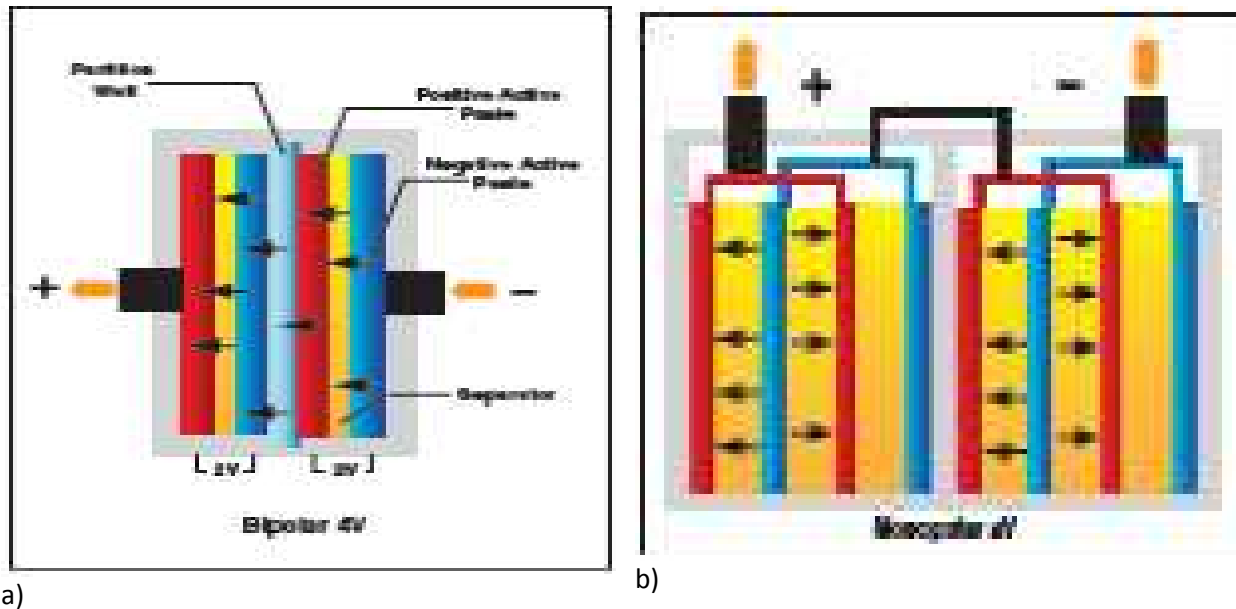
Figure 3: Bipolar design of lead-acid batteries.[37]

LABs with bipolar plates have a shorter current path, larger surface area, and higher power density than conventional monopolar designs of LABs. Each end of the LAB stack performs as the anode and cathode. The companies Atraverda (UK) and Effpower AB (joint venture of Volvo and Gylling Optima Batteries AB) have commercialized bipolar LABs. Effpower uses lead-infiltrated ceramic (LiC) plates. The AGM valve-regulates lead-acid (VRLA) batteries (AGM VRLAB) hold the electrolyte in glass mats in comparison with flooded LABs

The chemical overall reaction in AGM VRLA battery for discharge and charge is given below:

$$Pb + PbO_2 + 2H_2SO_4 \leftrightarrow 2PbSO_4 + 2H_2O \qquad (1)$$
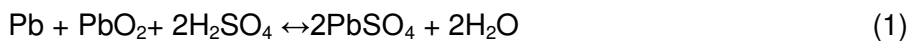
During discharge, the lead of the negative electrode (active material) and the lead dioxide of the positive electrode are transformed into lead sulfate and water. The formation of water shows that the acid concentration is decreased. During the battery's charge these processes take place in the reverse direction. Oxygen cannot move to the negative electrode in a flooded LAB, and its bubbles leave the electrode and escape through the vent plug. The VRLA-battery has the recombination of oxygen in its charging phase in which it moves through the pores of AGM or gel cracks to the negative electrodes. The cycle starts at the positive electrode:

$$H_2O \rightarrow \tfrac{1}{2} O_2 + 2H^+ + 2e^- \qquad (2)$$

Water is decomposed and oxygen is formed. Electrons move away via the positive electrode to the negative electrode, and the following reactions take place[38]

$$Pb + \tfrac{1}{2} O_2 \rightarrow PbO \qquad (3)$$

$$PbO + 2H^+ + SO_4^{2-} \rightarrow PbSO_4 + H_2O \qquad\qquad (4)$$

$$PbSO_4 + 2e^- \rightarrow Pb + SO_4^{2-} \qquad\qquad (5)$$

Oxygen oxidizes lead to lead oxide (reaction 3). This lead oxide is further transformed into lead sulfate with the participation of protons and sulfate ions (reaction 4). It is similar to a discharge process. Further products of this reaction are water and heat, in addition to the ohmic losses during charging; thus, the oxygen is recombined, water is re-converted, and the circle is closed. During the charge process the lead sulfate constantly reconverts into lead (reaction 4) on the negative electrode without the hydrogen evolution reaction. However, if hydrogen evolves at high charge currents and temperatures, it can't be reconverted due to the absence of hydrogen recombination. Hydrogen diffuses through the cell container and valve, which leads to water loss. Thus, the negative electrode doesn't fully charge. Hydrogen also evolves when negative grids corrode. In normal conditions, hydrogen is the main gas accumulated in the VRLA AGM battery; the VRLAB-design eliminates spills and off gassing.

The woven glass fibers of the negative electrode of an AGM VRLA battery increase its surface area

The AGM VRLA battery has significant advantages over conventional and gel lead-acid batteries:[39-42] (1) increased cycle life time (700 cycles), (2) better design for the deep discharge and charge cycles (important for high-rate-partial-state-of-charge (HRPSoC) for battery-electric locomotives), (3) 3-5 times less self-discharge, (4) "acid-starved" design that protects plates from fully discharging, (5) effective gas recombination is more efficient (99% AGM), (6) 100% maintenance-free, (7) AGM material has low electrical resistance, thus the battery delivers much higher power, (8) AGM batteries are rated at 100% of their capacity for charging and discharging amperage vs 35% for gel and flooded models, and (9) less acid means a lighter battery.

In contrast to AGM VRLAB, the gel VRLAB is more expensive and has shorter run-time and requires a special charger. VRLA batteries for the HEV application should operate within 30-70% SoC, but in reality they cannot provide the required cranking current at an SoC below 30% due to sulfation of their negative plates, insulation of non-conductive lead sulfate from lead grids, and difficulty of their recharge. $PbSO_4$ significantly decreases the active surface area of negative electrodes, limiting the battery's ability to provide power during acceleration and regenerative braking when it has a high rate of charge/discharge. This is determined by both the sulfation of negative plates at high-rate discharge and the early hydrogen evolution reaction at high-rate charge. Both of these processes reduce the battery's energy efficiency. The main solutions to these problems are as follows:

- localization of the charging current in plate surface at the high-frequency pulses[43]
- reduction of plate thickness and addition of carbon for even lead sulfate distribution[44]

Lead-acid carbon technology has a high rate of charge and discharge. This characteristic allows the lead-acid carbon batteries to deliver and accept high current rates that are only available for metal-hydride (Ni-MH) and Li-ion batteries. Different lead-carbon batteries have been developed by CSIRO,[40,41,44] Axion Power International,[45] and Xtreme Power.[46]

2.2.2 Asymmetric Super Capacitor-Based Hybrid Battery (PbC®(Axion Power International Inc.)

The electrochemical asymmetric supercapacitor (ASC) or hybrid energy storage (HES) will be analyzed in this section. The first ASC was ASC C/NiOOH/KOH.[47] Another ASC, $C/PbO_2/H_2SO_4$, was patented and commercialized by Axion Power International Inc.in 2001.[48-50] In contrast to the conventional lead-acid battery, the PbC® battery doesn't have any chemical reactions on the porous carbon negative electrode, and its energy storage is realized by a double layer (non-faradaic) storage determining its fast charge rate, and probably, proton pseudocapacitance (faradaic) storage. The PbC® battery has the same reactions on PbO_2 and the same positive electrode as a conventional LAB, with the reduction of PbO_2 to $PbSO_4$ and water formation during discharge and a converse reaction when charging. However, in contrast with a conventional LAB, the PbC® battery's negative electrode, which consists of activated carbon, doesn't have chemical reactions and adsorbed protons The negative electrode of the PbC® battery has a high surface area and more complex design and has five layers, namely: 1) a carbon electrode, 2) a corrosion barrier, 3) a current collector, 4) a second corrosion layer, and 5) a second carbon electrode. This electrode is assembled with the separator and the positive PbO_2 electrode forming a single PbC® cell, and several of them connected in a series form the PbC® battery. The positive electrode of the lead oxide-carbon ASC stores and provides Faradaic energy and provides longer cycle life and stable voltage. Additionally, employing a valve-regulated design, absorptive glass mat separator, starved-electrolyte configuration, and valve-regulated design increases the efficiency of the oxygen recombination cycle. The stability of the positive electrode's voltage increases the negative electrode's capacitance. A significant improvement in the performance of C/lead-acid HES was achieved due to the incorporation of lead into the carbon electrode with 200-600 mg/cm^2.[49,50]

PbC® batteries have several advantages over advanced lead-acid batteries: [51]

- Support higher [10-20x] charge acceptance
- Faster recharge [5-10x] in partial state-of-charge (PSoC) applications
- Offer 4x increase in cycle life in 100% depth-of-discharge applications
- Sustain 80-85% round trip efficiency in PSoC applications; 90-95% in deep cycle applications

It has been reported that the PbC® battery has the following advantages over Li-ion batteries: (1) twice higher cycle-life, (2) less energy cost/cycle $0.38 $/kW/cycle vs.1.2 $/kW/cycle, (3) less energy cost $600/kWh vs $1200/kWh, and (4) less recycling value at end-of-life of $35/lbs vs. $75/lbs.[52] The comparison of PbC®, Li-ion, and nickel-metal hydride batteries also shows that the PbC® battery has the potential for use in applications with high power output (rapid charge rate, long cycle life) (Table 1).[52] The PbC® battery is more cost effective compared to the Li-ion battery at the different duration of frequent discharge   (Table 2).[53]

Table 1: Comparison of the performance of PbC® e3 Supercell, Li-ion battery, and nickel-metal hydride battery (NiMH)[53]

Battery	Energy density (Wh/kg)	Battery cost ($/kWh)	Cycle life (cycle)
PbC® (e^3 Supercell)	12	600	1600
Nickel metal hydride battery	45	900	600
Lithium-ion battery	65	1200	1000
Lead-acid battery	25	250	400

Table 2: Present worth cost $/kW for PbC® and Li-ion batteries in 10-year operation in the first year[54]

Battery feature/Technology	Lead-acid carbon (PbC, Axion)	Li-ion
Long duration frequent discharge	2017	2899
Long duration infrequent discharge	1559	2442
Short-duration frequent discharge	669	1409
Short-duration infrequent discharge	825	960

Norfolk Southern has been using high-performance PbC batteries for all-battery switchers and working on line-haul hybrid locomotives since 2012 due to their high charge acceptance, fast charge and discharge capabilities (important in regenerative braking), and inherent ability to equalize voltage when utilized in large-string configurations.[54]

 The PbC® battery has a higher cycle life (1600 cycles at the charge/discharge cycle of 7h and 90% depth of discharge) than the conventional lead-acid battery (300-500 cycles) due to the absence of the sulfation of negative electrodes and lower levels of corrosion of the lead-alloy-based grids of positive electrodes at lower electrolyte concentrations. Neutralization of protons during discharge is due to their movement from the fully charged negative to positive electrode. PbC® with the patented e3 Supercell design has the following advantages over conventional lead-acid batteries:[52]

- Increase of the PbC® battery cycle life with use of the absorbed glass mat separator, a starved-electrolyte, and valve-regulated design similar to VRLAB

- Less corrosion of the lead grids of positive electrodes at dilution of sulfuric acid at the moving of protons from the negative to the positive electrode and with their subsequent neutralization to form water
- Reduction of mass shedding on the positive electrodes
- Elimination of premature negative electrodes caused by sulfation
- Reduction of premature failure due to the electrolyte's drying out as a result of the recombination efficiency of oxygen on the negative activated carbon electrode
- 65% less lead and battery weight compared with lead-acid batteries
- Longer life cycle in deep discharge applications
- Higher power rate
- Faster recharge rate

However, the PbC battery has less energy density (12 Wh/kg) than the lead-acid battery, which has 25 Wh/kg (Table 1)[52].

2.2.3 Hybrid Lead-Acid-Carbon Battery (UltraBattery® (CSIRO))

The hybrid lead-carbon battery (HB) is another type of advanced lead-acid battery that was developed and patented by CSIRO (Australia).[55] This battery, known as the UltraBattery® (UB), consists of a positive electrode (PE) PbO_2 and hybrid negative electrode (NE), which consists of connected LAB negative Pb electrode and ASC carbon electrode in parallel, AGM as the separator impregnated by sulfuric acid (Figure 4).[56.]
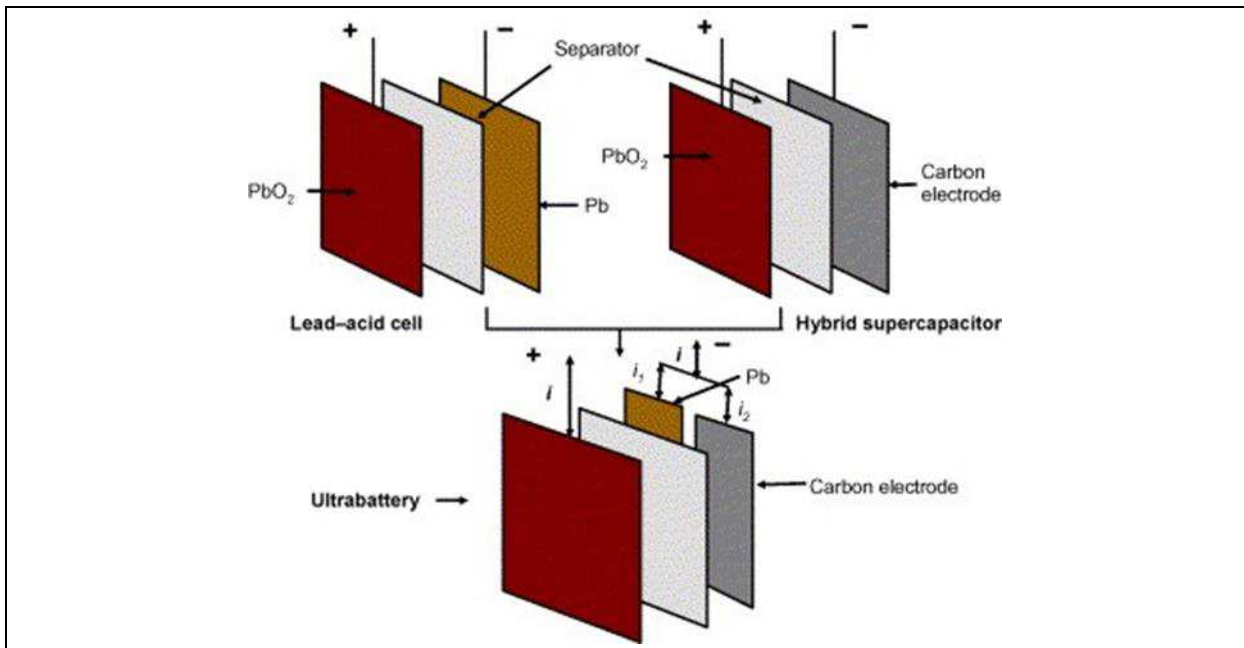
Figure 4: Configuration of UltraBattery® (CSIRO)[56]

This UB design presents a solution to the main problem of LABs, sulfation of NEs, particularly at the high rate partial state-of-charge (HRPSoC), and enables significant improvement of its cycle life, charge acceptance, and capacity compared to traditional LABs. The UB uses flooded and valve-regulated LAB design. The improved UB performance is determined by the lower internal resistance of the ASC carbon electrode, and as a result, it will first absorb and release charge during HRPSoC.[56] Therefore, a negative ASC carbon electrode plays the buffer role in UB to share the discharge and charge currents with the lead-acid negative electrode, protecting the latter from degradation at high discharge/charge rates and increasing its cycle life. Moreover, the carbon electrode has a PbO inhibitor of the side hydrogen evolution during the battery's charge, improving the UB's efficiency.

An additional advantage of the UB is determined by its high carbon content (2 wt.%) and, as a result, the formation of a conductive network between lead sulfate particles on the NE. This enables a decrease in the formation of the non-conductive lead sulfate, blocking the active surface area of NEs, and an improvement in the porous structure of NAM.[57-66]

In a comprehensive patent application, Lam et al have described a variety of combinations in which the negative and positive electrodes of Pb-acid batteries and asymmetric supercapacitors may be connected to form a hybrid energy storage device.[71] According to Lam et al, to suppress the side hydrogen evolution reaction, the ASC's negative electrodes contain additives, including, preferably, lead oxide.[67]

The main issue of the UltraBattery® is the different operational voltage of the two parts of its negative split electrode. For example, during the battery's discharge, the oxidation of lead to lead sulfate occurs at the potential of -0.98 V (SCE) on the LAB's negative electrode, charge neutralization occurs at voltages of more than 0.5V (SHE), and charge separation occurs at -0.3V (SHE) during the battery's charge (Fig.5).[67]

Therefore, during discharge the current comes mainly from the lead-acid negative electrode with the smaller portion coming from the capacitor negative electrode, and this portion increases at the end of the discharge. However, the main current first comes to the negative capacitor electrode at the beginning of charge and then to the negative lead-acid electrode. This leads to the side hydrogen evolution reaction on the negative lead-acid electrode, and it could be reduced by adding hydrogen inhibitors to the carbon electrode to reduce the hydrogen evolution reaction (HER) on it to the level of HER on the negative lead-acid electrode.
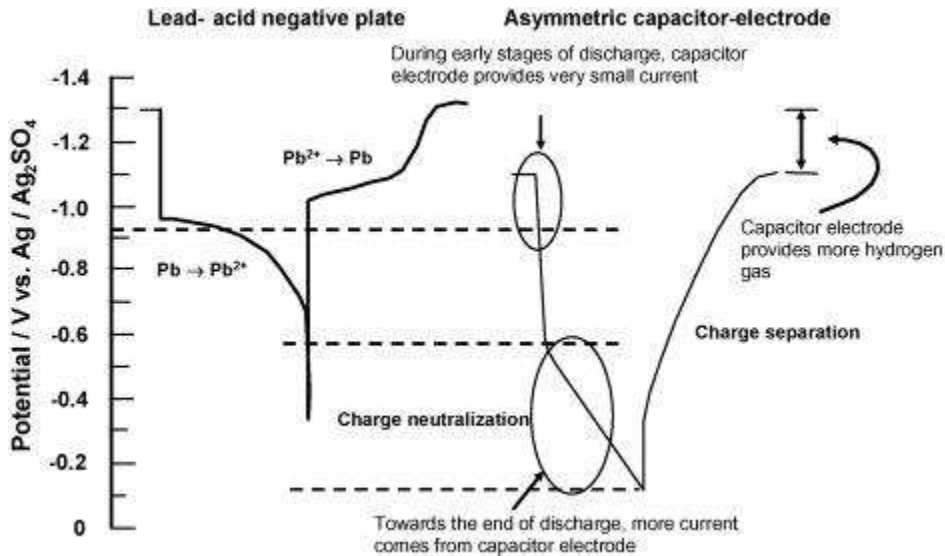
Figure 5: Operational potentials of a lead-acid negative plate and a carbon-based capacitor electrode during discharge and charge.[67]

Thus, the UB's innovative design and architecture give it a more advanced performance (cycle life, charge acceptance, cost efficiency) than LABs, NiMH batteries, and LIBs. The charge/discharge characteristics of the UB compared with the traditional LAB are shown in Figure 6. The UB capacity was improved by decreasing sulfation (formation on non-conductive film of $PbSO_4$) of NEs and blocking the active surface of NEs. The capacitor included in the UB is intended to increase the power and lifespan of LABs as it plays a buffering role during high rate of charge or discharge events. Examples of this are when the capacitor provides or absorbs charge quickly during hybrid electric vehicle acceleration and regenerative braking manoeuvres. UltraBattery® provides the following significant advantages:

- Performance combining fast charge from the supercapacitor technology with the concentrated energy of a lead-acid battery
- Longer cycle life (tens of thousands to millions of PSoC cycles depending on the cycle range of charge)
- High performance and efficiency for both power and energy applications
- Faster charging
- Advanced performance for UB-based HEV with a driving mileage of 100,000 miles/charge
- Safety and full recyclability
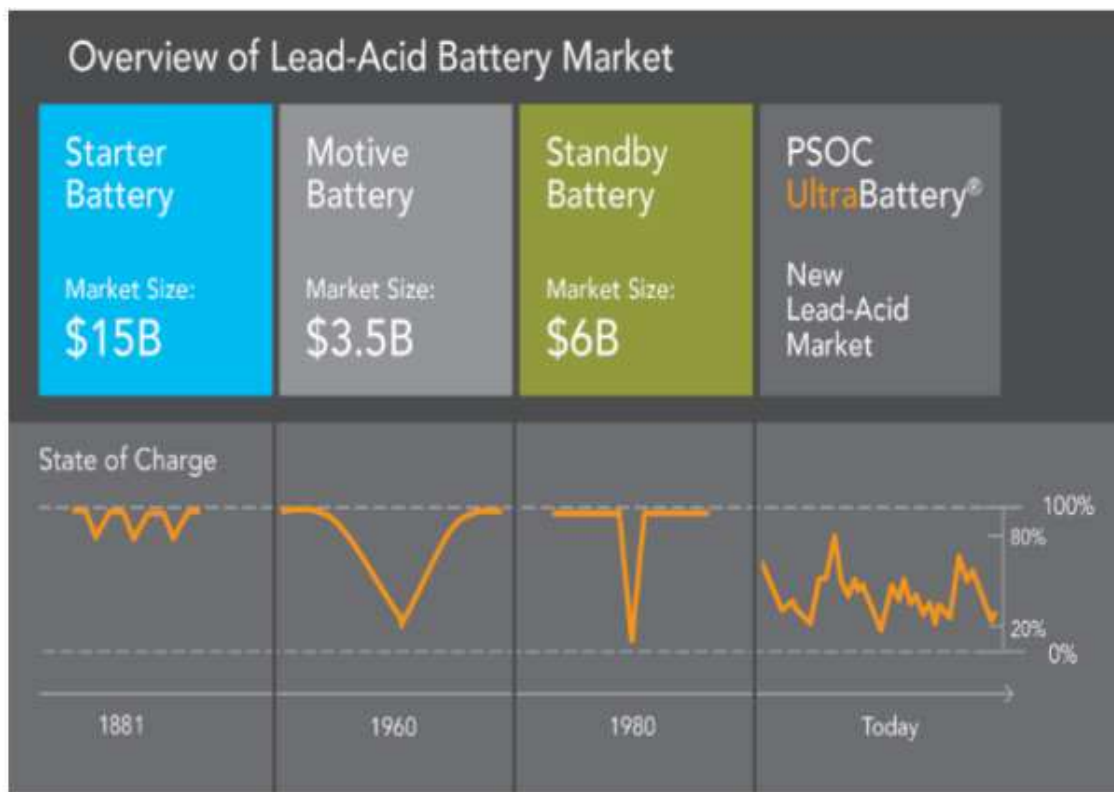
Figure 6: History of lead-acid battery technology[68]

In reviewing patent literature, CSIRO has claimed several designs of negative electrode for UB's, including the deposition of NE and ASC electrode pastes on opposite sides of Pb foam (electrode current collector), and the deposition of two layers of NE and ASC electrode pastes on one side of Pb foam , and only NE paste on the other side of Pb foam. [67]

The capacitor electrode consists of 20% carbon black with the specific surface area of 60 m^2/g (Denki Kagaku, Japan), binder (7.5% carboxymethyl cellulose + 7.5% neoprene), and 65% activated carbon with the specific surface area of 2000 m^2/g (Kuraray Kemikaru Co. Ltd, Japan).[67]The LAB's lead-containing paste (NAM) comprises leady oxide -1000g (83.7wt%), fiber 0.6 g (5wt %), carbon black -0.26 g (2.1wt%), $BaSO_4$ - 4.93 g, H_2SO_4 (1.4g/cm^3) - 80g, and water -110 ml; 4% sulfuric acid to leady oxide ratio, and paste density 4.2 g/cm^3.[66,67] The leady oxide was converted into lead oxide (PbO_2) and lead (Pb) during formation of NEs.

The UB's main benefits are the long cycle life and higher capacity turnover under cycling operations at PSoC.

Longevity Tests

There are two main types of longevity tests for UBs for applications with low (each cycle lasts for some minutes with small DOD) and high rates compared to 1C rate. The high rate test represents "balancing applications", such as HEVs and renewable energy smoothing. Low rate tests are mainly related to energy storage applications. A battery usually reaches the end of its life at the reduction of its capacity to 70-80% of its nominal life. The UB exceeds

the cycle life of traditional lead-acid batteries (Figure 7)[68] and Li-ion batteries (Fig.8).[73] The UB's cycle life is seven times longer (the cycle life of 5000 full capacity tests) than that of the AGM VRLAB after cycling at 1C, remaining at 100% of initial capacity (the VRLAB's capacity decreased 80% after 2500 cycles) (Figure 7). The UB has a better cycle life than the Li-ion battery.

The sustainability of UB for hybrid electric vehicles was demonstrated in an HEV Honda Civic with the UB pack providing a driving range of 160,000 km/charge. The laboratory test of UB in simulated conditions of the operation of medium-HEV at 60% SOC demonstrates the cycle life of 40,000 cycles that is 10 times longer than that of a conventional LAB.[68]UB has several advantages compared with the main NiMH battery:

- 70% less expensive
- Faster charge/discharge
- High Efficiency

UB has the typical DC-DC efficiency of 93-95% at its usage in regulation services applications. (Figure.9). The main applications of the UltraBattery® technology are as follows:[68]

- Micro- and medium-HEV hybrid electric vehicles (Honda Civic HEV-100,000 miles/charge)

Figure 7: Discharge voltage as a function of the number of cycles (EUCAR cycle life test at SOC and 2hr capacity

16
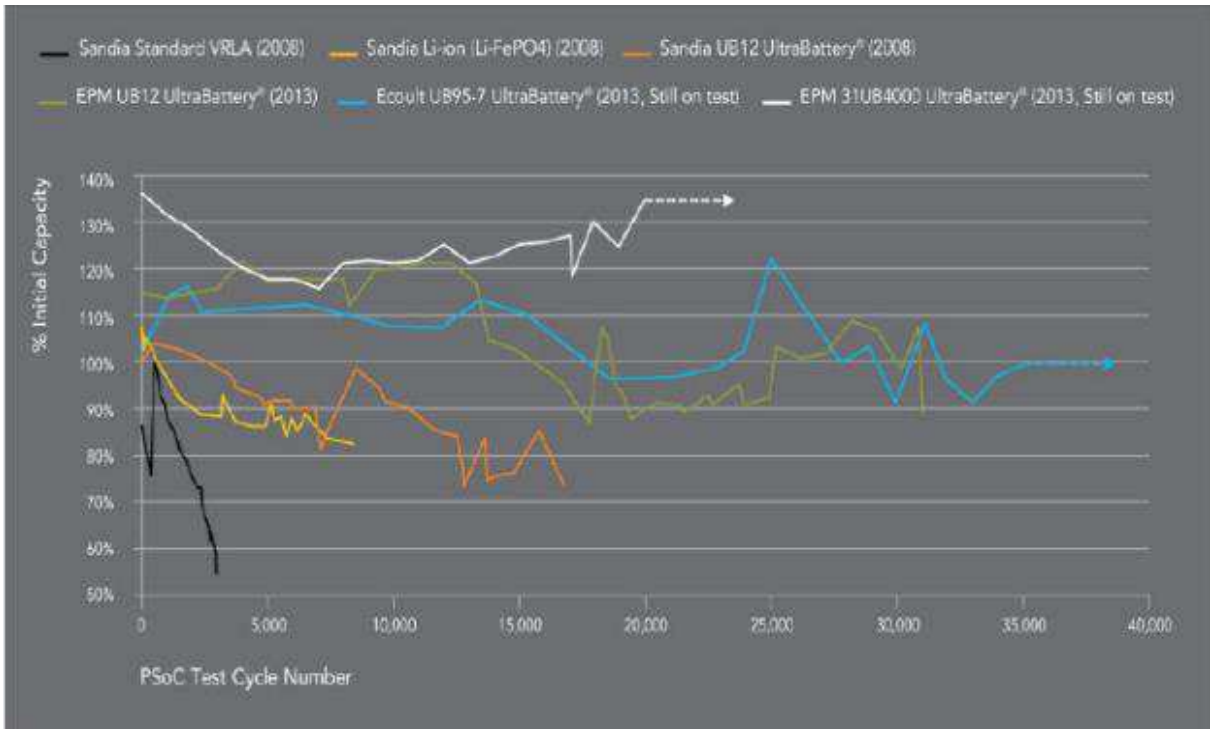
Figure 8: Longevity test of VRLA battery, Li-Ion battery, and UltraBattery for regulation service application PSoC[68]

Battery energy storage with high power output capability for railways (electricity distribution network operating in parallel with grid supplying)

- Energy storage technology in smart grids (i.e.: for smoothing wind farm output)
- Utility cycling applications (for PSoC cycling at different rates 1C to 4C)

The main benefits of UltraBattery® compared to lead-acid batteries are as follows:

- Lower life cost per kWh
- Better charge acceptance (quicker recharging)
- Lower maintenance
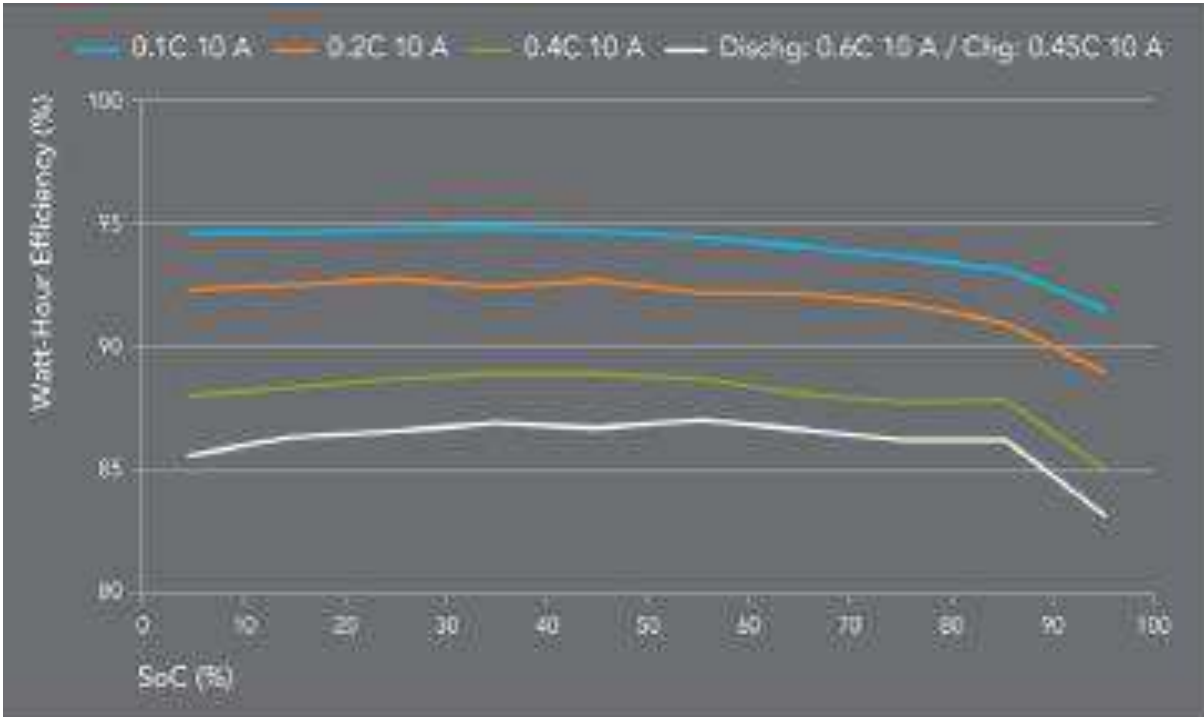
Figure 9: Efficiency (Wh) of UltraBattery PSoC and different C rates 0.1C, 0.2C, 0.4C Discharge at 0.6C, 10A. Charge at: 0.45C, 10C.[68]

3 DEVELOPMENT OF DESIGN AND MATERIALS FOR ASYMMETRIC SUPERCAPACITORS (ASC)

3.1 Baseline System Selection of Supercapacitor

The determination of a baseline supercapacitor cell is critical for assessing its commercially available components, which will ensure the supercapacitor's functionality as part of hybrid battery negative electrodes in the next phase. It was decided that the baseline cell would be a carbon-based supercapacitor, as this is the main type of supercapacitor found in the market.

Conventional components of a supercapacitor were then determined, purchased, and shared among the phases. These include:

- Stainless steel or lead foil current collectors
- Microporous Teflon sheets from W. L. Gore as separators
- YP80 carbon from Kuraray as activated carbon
- Super C45 from Timcal Canada as the conducting carbon additive of the active layer

The formulation of the active layers paste is of prime importance for the reproducibility of the results. The activated carbons used to store the energy are generally not good electrical conductors, which limits the power output of the system. A selected amount of conductive carbon (carbon black, graphite, or more recently, carbon nanotubes) is thus mixed with the activated carbon to increase the conductivity, and avoid this limitation. A number of companies in the lithium-ion industry use a polyvinylidene fluoride (PVDF) binder to turn the active material powders into a paste and bind them to the current collectors. However, the use of an important quantity of PVDF is required to ensure good mechanical properties (10-15 wt%). PTFE is also used as a binder in the industry. It has the ability to bind the powders very efficiently, even at very low content (typically 5 wt%). Because of its higher performance long-term, the PTFE binder was selected for this part of the study. As a baseline active material paste, it was chosen to use:

- 80 wt% of YP80 activated carbon
- 15 wt% of C45 carbon as conductive additive
- 5 wt% of PTFE binder

Two current collectors were chosen for the characterization baselines:

- 300μm in thickness of stainless steel (AISI 316)
- 700μm in thickness of the lead foil

The electrolyte 1.28 g/cm^3 sulfuric acid used in the traditional lead-acid battery was chosen for the characterization baseline cells.

3.2 Supercapacitor Lab-Test Cell

An NRC home-made lab-test cell and an air-tight box were chosen for evaluation of the supercapacitor. Figure 10 shows several views of the NRC cell design.
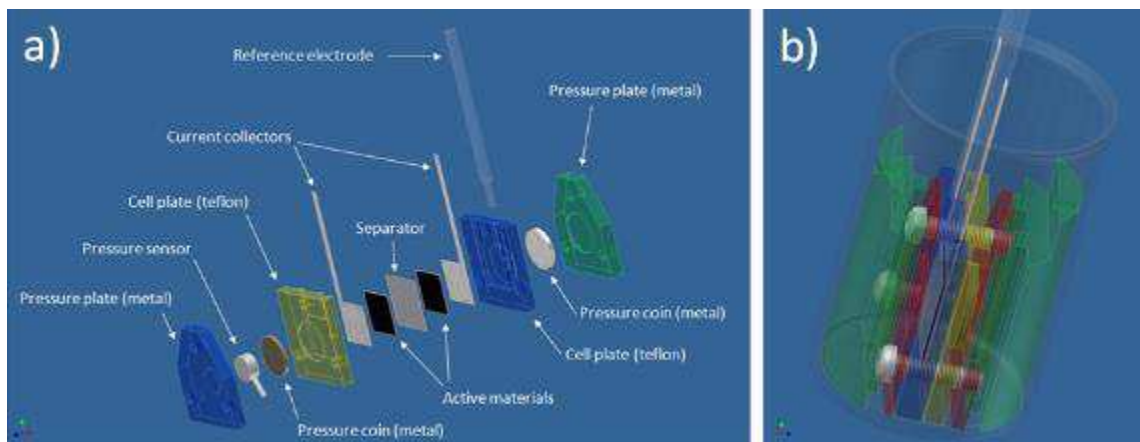
Figure 10: Design of the supercapacitor laboratory test-cell a) expanded view and b) assembled cell in its beaker with two Teflon fillings (in green) designed to decrease the amount of electrolyte needed to fill the beaker

The cell was designed for a cell stack size of 2 cm x 2 cm. The cell stack (active material pastes + current collectors + separator) is assembled in a compartment carved in one face of the two Teflon plates (Figure 10a, left), and the size is 2.05 x 2.05 cm. At each corner of the compartment, a small hole has been carved for a suitable folding of the separator sheet (which has to be bigger than the compartment size to effectively prevent short-circuits). On the opposite Teflon plate (Figure 10a, right), a block 2 x 2 cm^2 in size closes the stack compartment.

On the upper side of the stack compartment, two channels are carved for the electrical connections of the current collectors. The cylindrical compartment for the reference electrode is carved on the side of the stack compartment. A small channel at the bottom of this compartment connects the two compartments.

Figure 11 shows the test consisting of a) internal Teflon plates showing the compartment for the supercapacitor stack: current collectors, active materials and separator, as well as the reference electrode compartment, b) pressure system including two metallic plates with a three-point screwing design for an optimal pressure balance, as well as two metallic coins which effectively transfer the pressure to the internal cell compartment, and c) assembled cell showing the metallic current collector of each electrode protruding from the upper side and the reference electrode placed in its compartment.
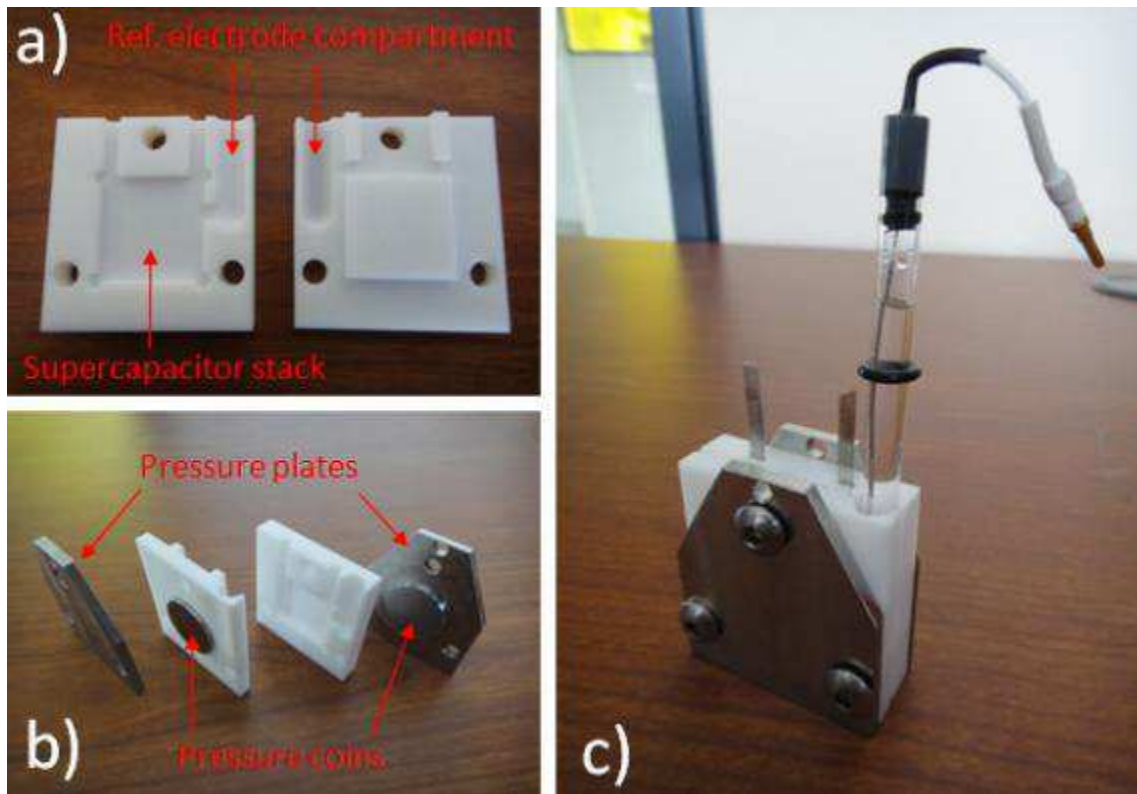
Figure 11: Photographs of the laboratory test-cell

Two metallic plates are placed on each side of the assembled cell and are screwed using a three-point geometry ensuring a better pressure balance than a four-point geometry. The pressure from the metallic plates is directly transferred to the supercapacitor stack through two metallic coins placed on the back of each Teflon plate of the internal cell (Figure 11b).

The test-cell was designed to allow the optional addition of a pressure sensor (Figure 10a). This will allow very precise control of the pressure applied to the cell with the screws, and refine the pressure application procedure. This will also allow the study of the variations of the stack pressure during cycling.

The complete set of components is show in Figure 12. The beaker volume is 100 mL, but two Teflon fillings (on the upper left corner of the Figure) have been designed to fill the volume not occupied by the cell (Figure 10b), in order to minimize the amount of electrolyte needed to ~ 20 ml.
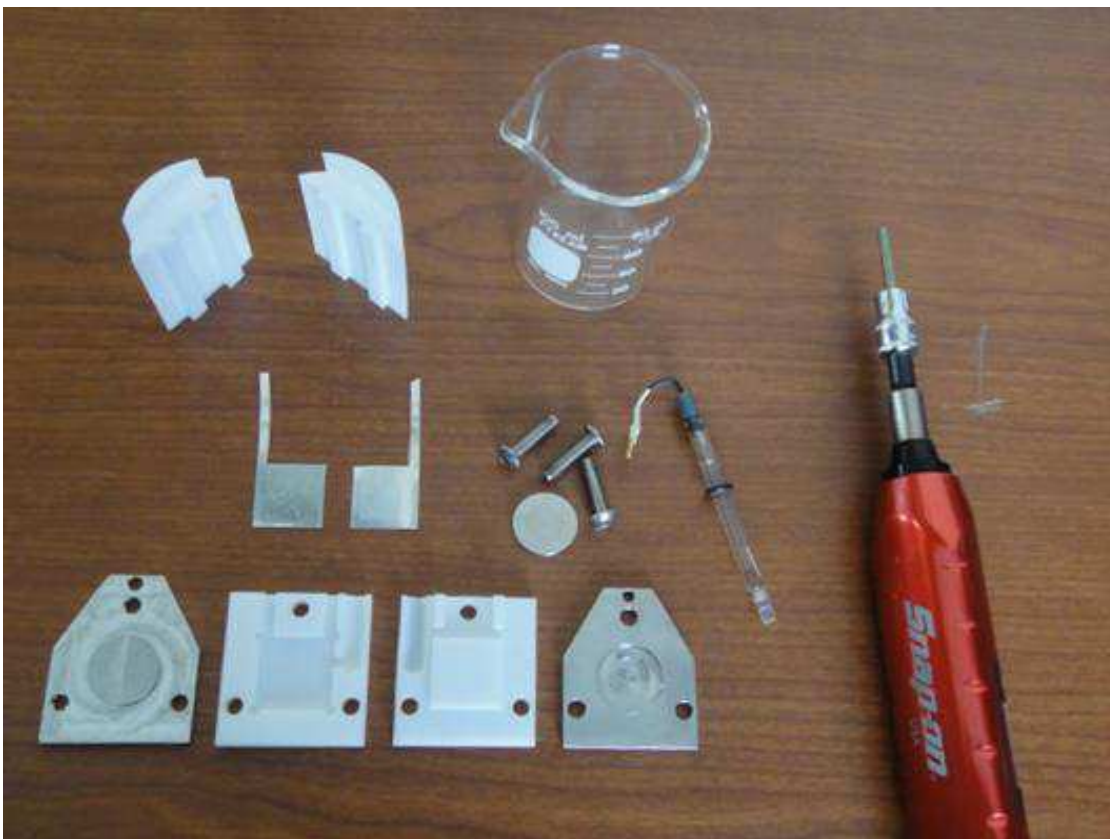
Figure 12: Photograph of a disassembled cell showing all components including the beaker, Teflon fillings and a dynamometric screwdriver used to control the pressure applied to the internal cell

3.3   Integration of Carbon Electrodes into the Baseline Supercapacitor and ASC

3.3.1 Preparation of the Baseline Active Layer Pastes and Electrodes

Different procedures can be found in the literature to turn the active material powders into a paste and bind them to the current collectors.

Depending on the active material, conductivity additive, and binder used, the weight ratio of active material, additive and binder ranged from 90-80:5-15:5-15. In this study, Kuraray YP-80, Timcal Super C45 and PTFE were used to prepare electrode layers for the baseline test. The composition ratio used was 80:15:5. The paste was prepared as follows:

1. YP-80, C45, and PTFE were first weighted, mixed, and ground together in a mortar
2. The mixtures were then transferred to a beaker and dispersed in ethanol under strong stirring
3. The PTFE binder was then added with more ethanol to the powder dispersion, and the temperature was raised to evaporate the solvent

22

4. After most of the ethanol had been removed, the paste was collected on a glass slide, where it was manipulated (mixed together) with a spatula to impart some mechanical cohesion
5. When sufficient mechanical properties were obtained from the wet paste, it was submitted to several cycles of rolling and folding to homogeneously disperse the PTFE fibrils in the paste
6. Cycles of drying in air and rewetting with ethanol may be necessary while the paste is being manipulated, as ethanol makes the PTFE fibrillate
7. When sufficient mechanical properties were obtained from the active layer paste, it was rolled to the required various thicknesses (in this formulation study, three thicknesses were tried, i.e., 115 µm, 250 µm and 850 µm) using side gauges, as shown in Figure 2.4.

Squares (8.2 cm x 2 cm) of active materials were then cut in the paste and placed in an oven at 120°C under an active vacuum (Figure.13b) overnight, weighed, and transferred as electrodes for assembly.
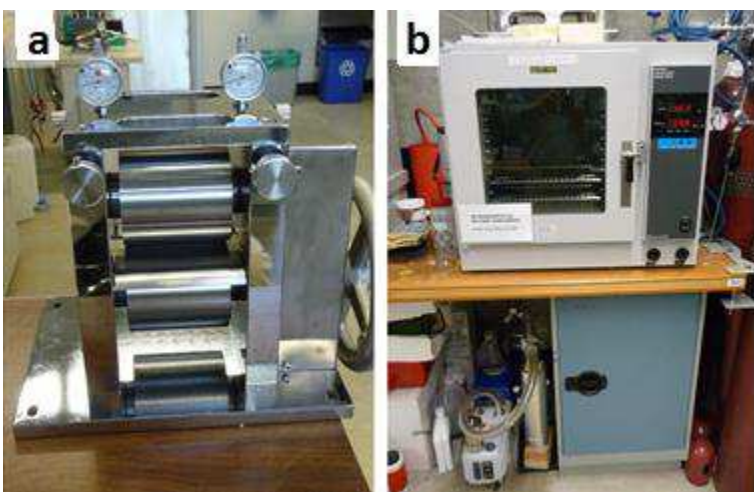
Figure 13: Photographs of a) rolling press and b) vacuum oven

3.3.2 Preparation of the ASC Active Layer Pastes and Electrodes

Active materials for the ASC in a hybrid battery system are commonly requested to add additives to prevent hydrogen gassing due to the mismatch between the cell's voltage and the potential range of the electrode. The common additives for hydrogen inhibition in hybrid lead-acid batteries are oxides. In this formulation study, lead oxide was chosen. The active materials for the ASC negative electrode in this work consist of:

- 80 wt.% of YP80 activated carbon
- 10 wt.% of C45 carbon as conductive additive
- 5 wt.% of PTFE binder
- 5 wt.% of lead oxide

23

One current collector was chosen for characterization of the ASC negative electrode:

- 300μm in thickness of stainless steel

The electrolyte medium was chosen for characterization of the ASC negative electrode:

- 1.28 g/cm^3 sulfuric acid

Preparation of the ACS active layer pastes and electrodes was as described in part 3.3.1

3.3.3 Assembly of Baseline Supercapacitor and ASC Lab-Test Cell

Proper assembly of the test cell was of great importance in order to ensure reproducible results. The parameters found to be critical are impregnation of the electrolyte by the active layer paste and the pressure applied to the cell.

Two electrodes (2 x 2 cm), made as in sections 3.3.1 and 3.2.3.2, and the separator were first aligned and laminated together, then dried in a vacuum oven at 80ºC for 6 hours. The sandwiched electrode and separator were then impregnated with electrolyte under vacuum before being assembled into a test cell. A few drops of electrolyte were added at each step of the test cell's assembly in order to ensure the presence of a proper amount of electrolyte in the core of the cell.

Control of the pressure is very important to reproducible results from the cells, thus pressure was applied to the test cell using a dynamometric screwdriver at torque 200cNm for the pressure screws to intimately bind the different layers of the stack. Figure 11c represents the assembled cell showing the metallic current collector of each electrode protruding from the upper side and the reference electrode placed in its compartment.

3.4 Electrochemical Test of Baseline Supercapacitor and ASC

Assessment of the baseline supercapacitor and carbon-based ASC performances is achieved using different techniques of electrochemical characterization.

A specific procedure was determined, including the following techniques:

- Cyclic voltammetry
- Galvanostatic cycling

These procedures allow for the determination of the main characteristics of supercapacitor and ASC: capacitance of the active materials, maximum voltage, and cyclability.

Cyclic voltammetry (CV) is one of the key techniques used for the electrochemical characterization of energy storage devices. The voltage (or potential, when looking at a single electrode) is progressively scanned back and forth at a constant rate between two limits, and the current response is recorded.

In galvanostatic experiments, a constant current is applied to the cells and the voltage response is baseline recorded.

3.4.1 Electrochemical Test of Baseline

The CVs of the baseline supercapacitor cells at various scan rates, with stainless steel and lead foil as the current collectors respectively, are presented in Figures 14 and 15. The capacitances calculated at different scan rates are shown in Tables 3 and 4 respectively as well.

It can be observed that the low scan rate curves are very similar, showing that both current collectors have similar properties, i.e., ideal supercapacitive behavior (rectangle shape). When the scan rate (power demand) is increased, a polarization phenomenon is observed in the lead foil current collector (Figure 15) with a progressive loss of the ideal behavior. This is most probably due to the higher contact resistance between the Pb foil and the carbon electrode, which deformed and caused loose assembly. Overall, at high scan rates, the cell capacitance is decreased for both current collectors because the rate of the voltage scan is too fast for the ions to insert and to leave the active layer effectively. This phenomenon is typical of carbon-based supercapacitors, and it limits both the energy output and the power output of the device.

The cycling performance of the baseline supercapacitor cells (stainless steel and lead foil as the current collectors) was also investigated using galvanostatic cycling. Figures 16 and 17 present a galvanostatic cycling (GC) of the two baseline cells. The capacitances calculated at different currents are shown in Tables 5 and 6 respectively as well. Both cells demonstrated the typical triangular shape of a carbon-based supercapacitor. The most noticeable difference is the time it took to charge and to discharge the cell, specifically at higher current, i.e., 100 mA. The Pb foil has higher contact resistance with the carbon electrode; its capacitance was lower than stainless steel, resulting in quick charge/discharge cycles. This is consistent with observations in CV curves.
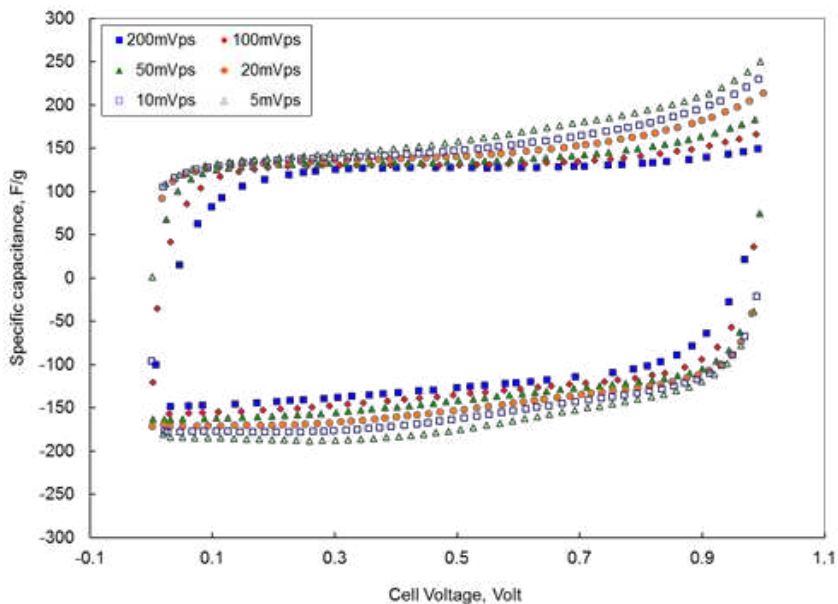
Figure 14: Cyclic voltammogram of the baseline cell (current collector: stainless steel, electrode thickness: 115μm) at various scan rates mV/s

Table 3: Capacitances calculated from Figure 14 at various scan rates mV/s

mV/sec	F/g
200	122.9
100	130.8
50	137.5
20	145.9
10	153.9
5	162.4
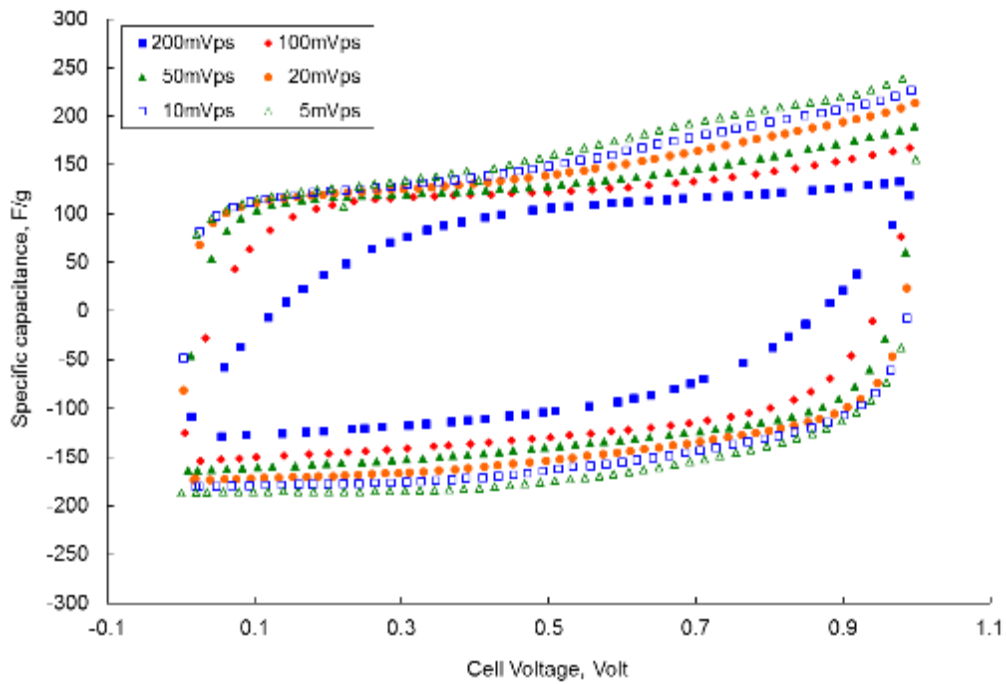
Figure 15: Cyclic voltammogram of the baseline cell (current collector: lead foil; electrode thickness: 115µm) at various scan rates mV/s

Table 4: Capacitances calculated from Figure 15 at various scan rates mV/s

mV/sec	F/g
200	101.5
100	120.8
50	132.7
20	144.7
10	153.2
5	162.7
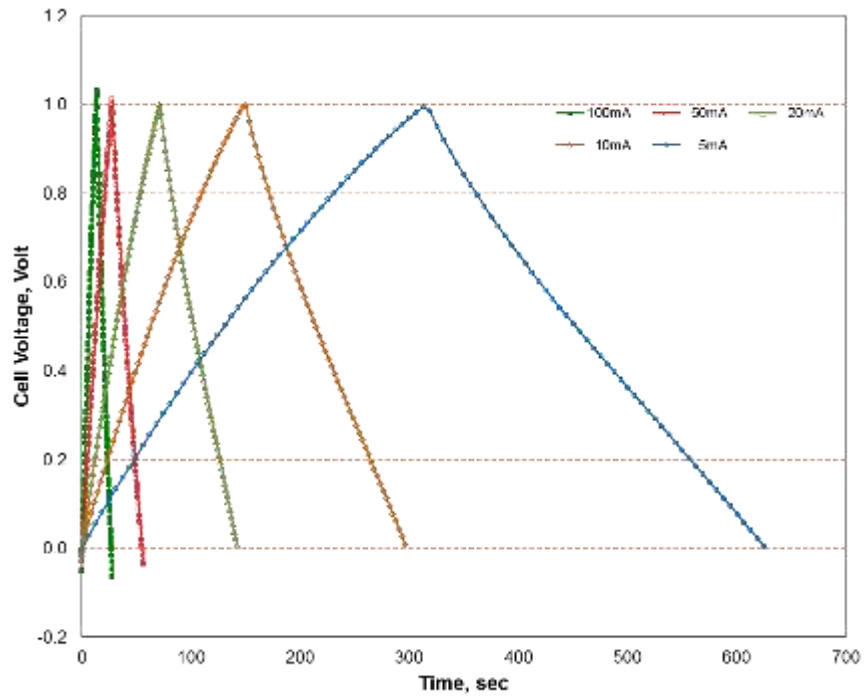
Figure 16: GC curves at different currents of stainless steel based cell

Table 5: Capacitances calculated from Figure 16 at different currents

mA	F/g
100	137.4
50	143.1
20	152.8
10	162.3
5	173.2
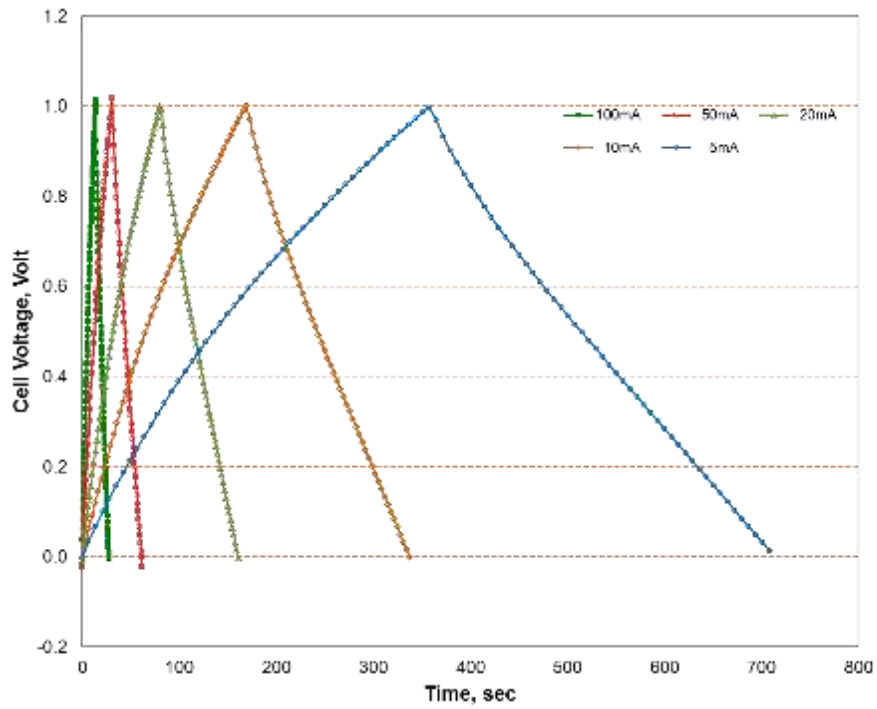
Figure 17: GC curves at different currents of Pb foil based cell

Table 6: Capacitances calculated from Figure 17 at different currents

mA	F/g
100	129.7
50	142.8
20	154.2
10	164.9
5	177.7

3.4.2 Electrochemical Test of Asymmetric Supercapacitor (ASC)

Usually, the thickness of the Pb grid used in a real lead-acid battery is around 2mm-3mm, which is one order thicker than that of carbon electrode materials used in a supercapacitor (max. 200μm). This mismatch will cause significant performance degradation. To solve this mismatch issue, separate electrodes with increased electrode thickness, i.e.: 250μm and 850μm respectively, were fabricated and tested in the ASC.

The CVs of two kinds of ASC carbon electrode thickness at various scan rates with stainless steel as the current collector are presented in Figures 18 and 19. The capacitances calculated at different scan rates are shown in Tables 7 and 8 respectively as well. In order to test the ASC in a real world application for transportation (power demand), the scan rates for both ASCs were increased to as high as 1000 mV/s. It can be observed that at lower scan rates (<200mV/s), both ASCs showed very similar capacitances, which were also similar to that of a baseline supercapacitor cell with electrode thickness of 115μm (see Table 5). However, when the scan rate was increased (power demand), the electrode with a thickness of 250μm had a better capacitance than the 850μm electrode, specifically when the scan rate reached 500 mV/s, most probably due to a thinner electrode layer that allows for easier ion diffusion.

Cycling performance of the ASCs (stainless steel as the current collector and two kinds of electrode thickness) were also investigated using galvanostatic cycling. Figures 20 and 21 show the galvanostatic cycling (GC) of the two ASC electrodes with different electrode thicknesses. The capacitances calculated at different currents are shown in Tables 9 and 10, respectively, as well. Both cells demonstrated the typical triangular shape of a carbon-based supercapacitor. Interestingly, contrary to CV observations, where at higher scan rates thinner electrodes (i.e.: 250μm thickness) showed less polarization and thus higher capacitance, the electrode with thicker thickness (i.e.:850μm) retained a good capacitance of ~145F/g even at a current of 1000 mA. Since the baseline supercapacitor and the ASC electrode with a thinner carbon layer both had much less material in their electrodes (115μm and 250μm in thickness respecttively), they had lower capacitances than the ASC electrode with a thicker carbon layer (850 μm) resulting in quicker charge/discharge cycles.

It is important to note that the increased thickness of the carbon electrode (as thick as 850μm) with an optimal electrode preparation and cell assembly protocols, could not only retain a good capacitance in a lead acid electrolyte environment, it also solved the mismatch issue between the thickness of the Pb grid used in real lead-acid battery and the carbon electrode materials used in a supercapacitor.

The results obtained showed that the optimal formulation is particularly promising for asymmetric hybrid battery negative electrode material research. Thus, the ASC electrode developed and validated in this phase could be successfully transferred into the next phase for lead-acid negative electrode integration.
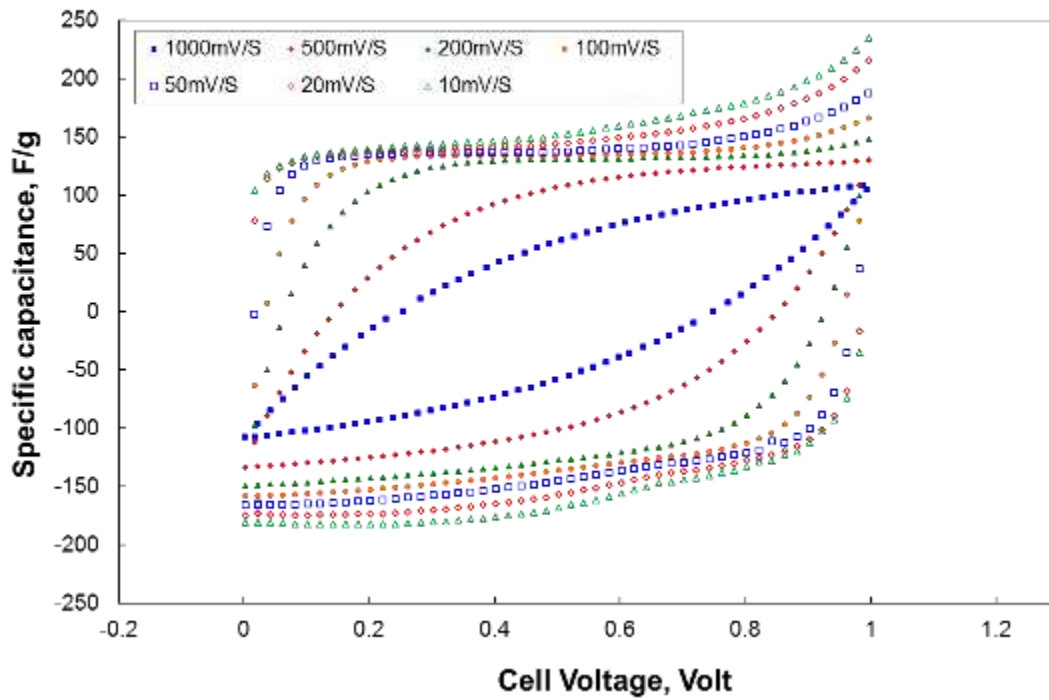
**Figure 18: Cyclic voltammogram of ACS (current collector: stainless steel, electrode thickness: 250 μm) at various scan rates mV/s**

Table 7: Capacitances calculated from Figure 18 at different currents

mV/sec	F/g
1000	70.9
500	100.5
200	121.1
100	131.2
50	140.0
20	150.2
10	158.5
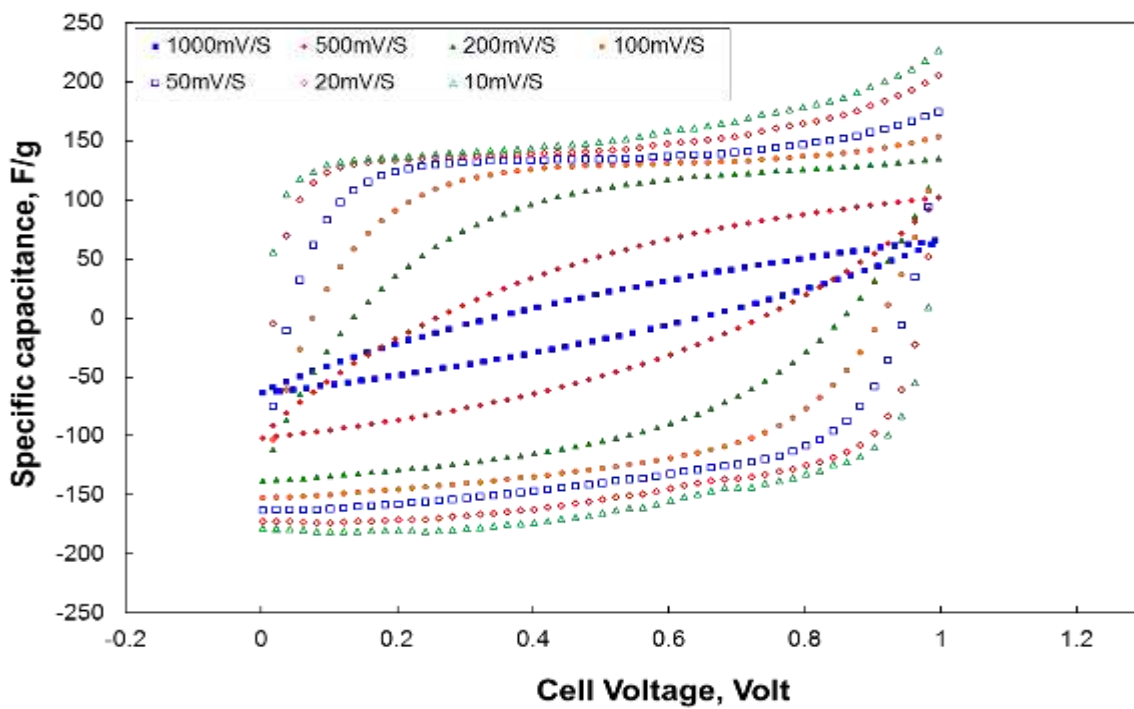
Figure 19: Cyclic voltammogram of ACS (current collector: stainless steel, electrode thickness: 850 μm) at various scan rates mV/s.

Table 8: Capacitances calculated from Figure 19 at different currents

mV/sec	F/g
1000	37.1
500	64.3
200	101.4
100	120.4
50	132.3
20	146.3
10	155.7
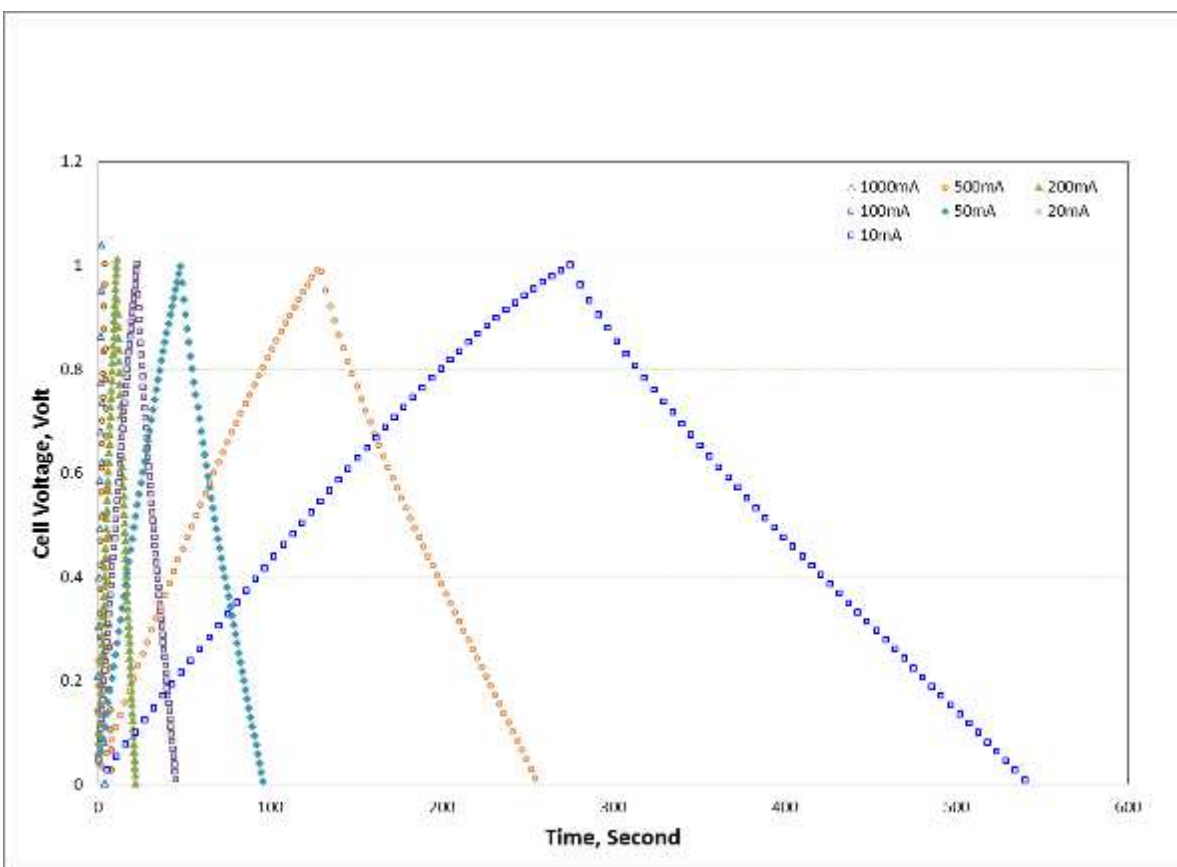
Figure 20: GC curves at different currents of ACS (current collector: stainless steel, electrode thickness: 250μm)

Table 9: Capacitances calculated from Figure 20 at different currents

mA	F/g
1000	121.1
500	129.9
200	137.7
100	143.6
50	151.5
20	163.2
10	177.8
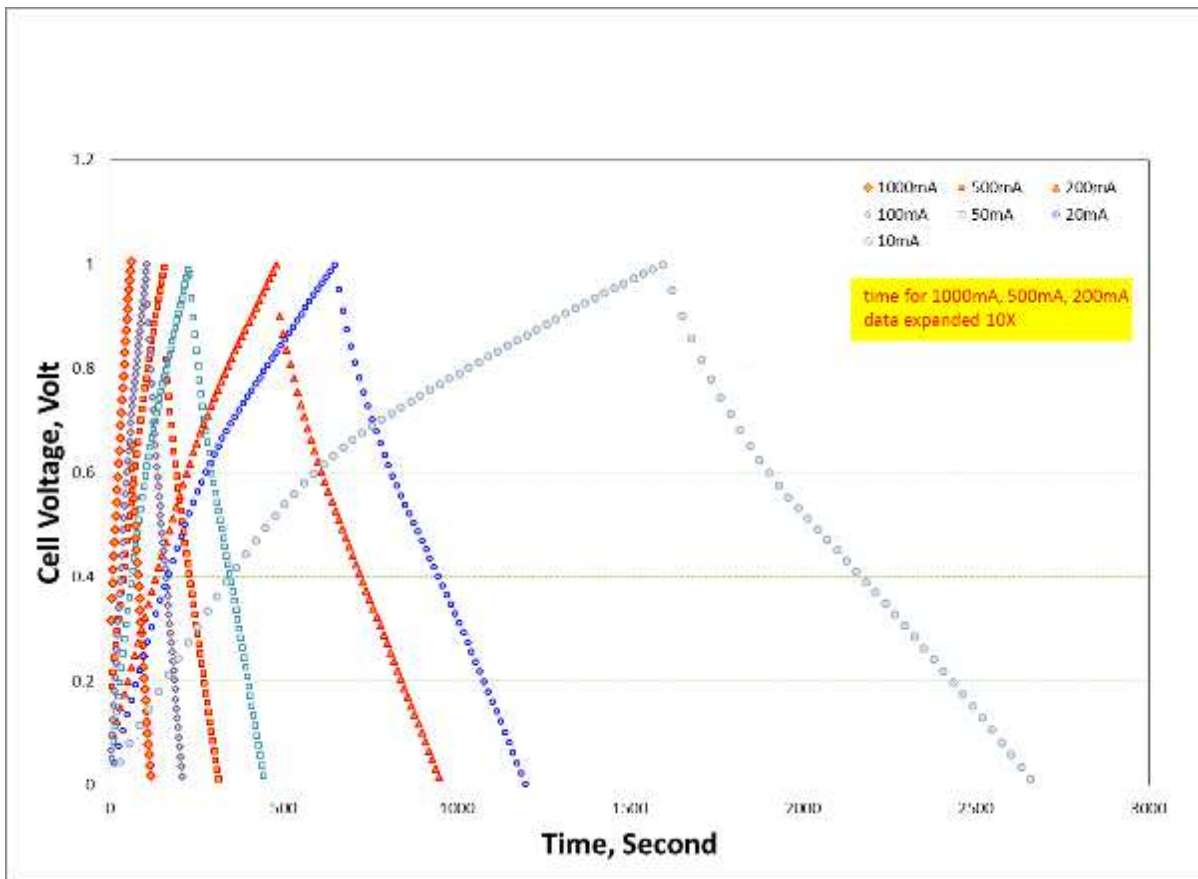
Figure 21: GC curves at different currents of ACS (current collector: stainless steel, electrode thickness: 850 μm).

Table 10: Capacitances calculated from Figure 21 at different currents.

mA	F/g
1000	145.8
500	159.1
200	189.4
100	206.2
50	217.7
20	222.0
10	212.8

4   DEVELOPMENT OF THE ADVANCED AGM VRLAB

4.1   Baseline System Selection of AGM LAB

The baseline AGM LAB (2V) was developed for the evaluation and comparison of the performance of AGM LABs and hybrid battery with homemade negative electrodes. It consists of the commercial (negative electrode (NE) with the carbon concentration of 0.15% and two positive electrodes (PE, 2.2 x 2.2 cm), absorption glass mat (AGM, Hollingsworth and Vose (USA)), and the electrolyte H_2SO_4 (1.28 g/cm^3). Given that one NE was measured to have less capacity than two PEs, this resulted in the overall performance of the baseline battery being determined by the NE. Dry electrodes were soaked in the H_2SO_4 (1.265 g/cm^3) electrolyte for 1h and electrochemically activated at 0.015A (current - 5% of C20 for 1h) in the electrolyte H_2SO_4 (1.28 g/cm^3). Negative electrode capacity for the baseline AGM LAB was of 0.25Ah.

The Surrette's positive electrodes were used in all test cells, including the hybrid battery. Their development was not rational due to small impact on the LAB performance

The calculation of NE's capacity is given below:

- One mole of Pb is equal to 207.2 g
- One mole of elementary charge [Faraday] equals 96485.34 Coulombs
- The oxidation of lead is a two-electron electrochemical reaction, and therefore 192970.68 Coul or 53.603Ah of charge will be theoretically transferred per mol of Pb (equal to 207.2g of Pb)
- Therefore, for a NE capacity of 0.25 Ah, 1,93g of Pb is required at 50% Pb utilization,

4.2   Development of AGM LAB's Electrodes

According to the analysis of state-of-the-art (SOTA) technologies, a mixture of the acetylene carbon black AB50 (the specific surface area of 75m^2/g) and conductive carbon additive (C45) (Figure 22) were used to decrease the sulfation of LAB's negative electrodes.
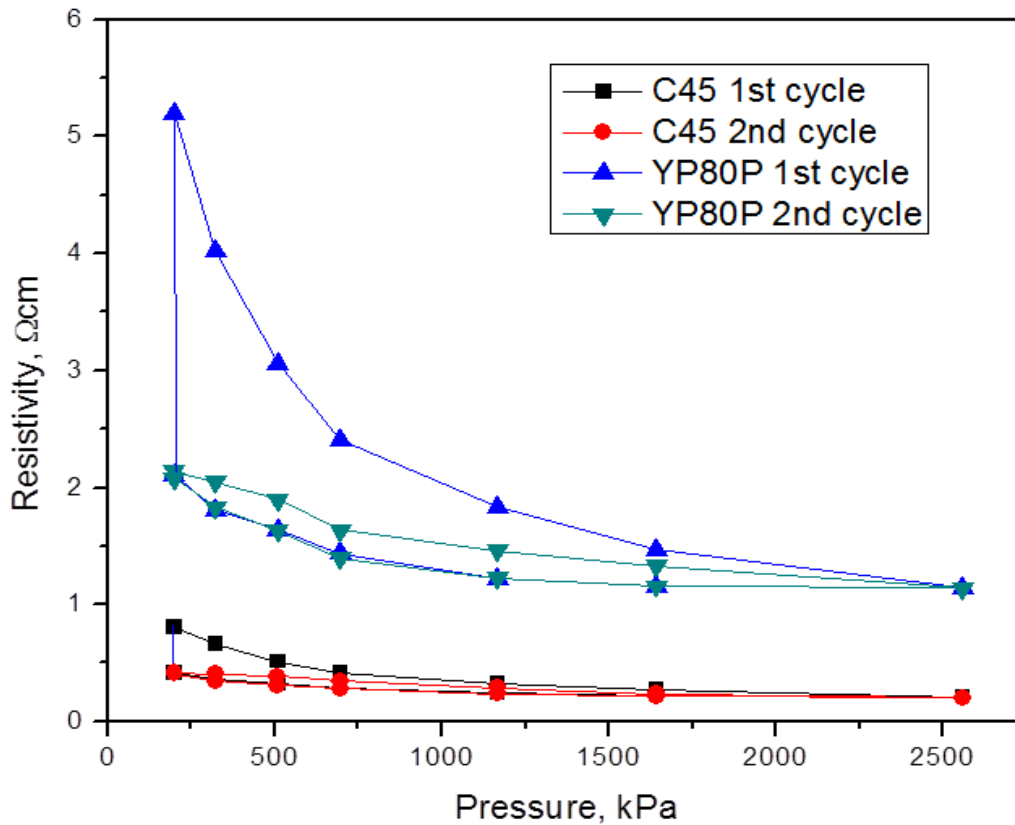
Figure 22: Resistivity of the carbon black C45 and YP-80.

One of the factors that substantially limits the cyclability of LABs operating at HRPSoC mode is sulfation of negative plates. During high-rate discharging, the Pb grids react with HSO^{4-} to form $PbSO_4$, which blocks diffusion of anions from a bulk solution. Moreover, a compact layer of $PbSO_4$ reduces the active surface area for electron transfer. A proposed hybrid AGM lead-acid cell with a new graded NE will be used in a hybrid railroad yard switcher locomotive operating at HRPSoC, when only a small fraction of its capacity is involved in the charge and discharge processes that occur continuously at a very high rate. During subsequent high-rate charging, complete conversion of lead sulfate on the NE surface cannot be achieved. With such repetitive action, $PbSO_4$ will accumulate and eventually cause degradation of the LAB.

Advantages of the addition of a high amount of carbon to NE are as follows:

- increasing the porosity of electrodes and penetration of the electrolyte
- minimization of the pore blockage by lead sulfate within the cross-section of NP
- formation of a conductive network among $PbSO_4$ particles
- impeding the continuous growth and deactivation of $PbSO_4$ crystals
- enhancement of the utilization ratio of active substances

36

- supplying a double layer and pseudo-capacitance during high rate processes (buffer action)
- reduction of the mechanical damage to NPs caused by high or pulse currents
- simplification of the surface area balancing between the negative and positive stack
- enhancement of the cycle performance of NPs under HRPSoC
- increase of the hydrogen evolution overpotential and decrease of H_2 evolution rate.

Disadvantages of the carbon presence in the negative electrode that should be addressed:

- hydrogen evolution during the charging process
- increased inner pressure
- accelerated water loss

The hybrid lead-acid cell with a negative electrode with the capacity of 0.25Ah is the baseline test cell for a cycling test at C rates less 1C and 50% SOC.

Fabrications of Negative Electrodes

The process of LAB's negative electrode manufacture consists of several stages:

> Paste preparation
>
> Pasting of lead grids
>
> Drying of paste
>
> Curing of paste
>
> Electrode formation
>
> Electrode drying
>
> Paste preparation
>
> Pasting of lead grids

The conventional composition of negative active material (NAM) paste was used in the negative LAB electrodes.[69]

A list of raw materials used for the NAM paste preparation is presented below:

- Sulfuric acid (Grade ACS, 17.8M, Assay 95-98%, Alfa Aesar). For negative electrode paste preparation sulfuric acid was diluted with H_2O down to 50 wt% or 1.4 g/cm^3. Solutions with 37% of H_2SO_4 (1.28 g/cm^3) have also been prepared for a further application
- Leady oxide (Surrette Battery Co.) contains 6-7% of Pb. It has been characterized by XRD (Figure 23) and SEM (Figure 24). The material contains synthetic tetragonal and orthorhombic PbO and the natural mineral massicot
- Conductive carbon black C45 (Timcal)
- Acetylene carbon black AB-50 (Chevron Co. $BaSO_4$, (99.9%, Alfa Aesar Co.)
- Vanisperse A (Borregaard LignoTech Inc.)
- Fibers (polyester) up to 0.01g (Goonvean)

Table 11: Composition of a NAM paste.

Negative electrode material paste	
Chemical	Weight, wt% (solid paste)
PbO (Barton pot leady oxide [Surrette Battery Co.])	71.5%
$BaSO_4$	0.7%
H_2O	12.2%
H_2SO_4	14.6% ($1.28g/cm^3$)
Vanisperse A	0.02%
Carbon * (*i.e. : AB50:C45=8:1)	0.9%
Fibers (polyester)	Up to 10% of total C amount
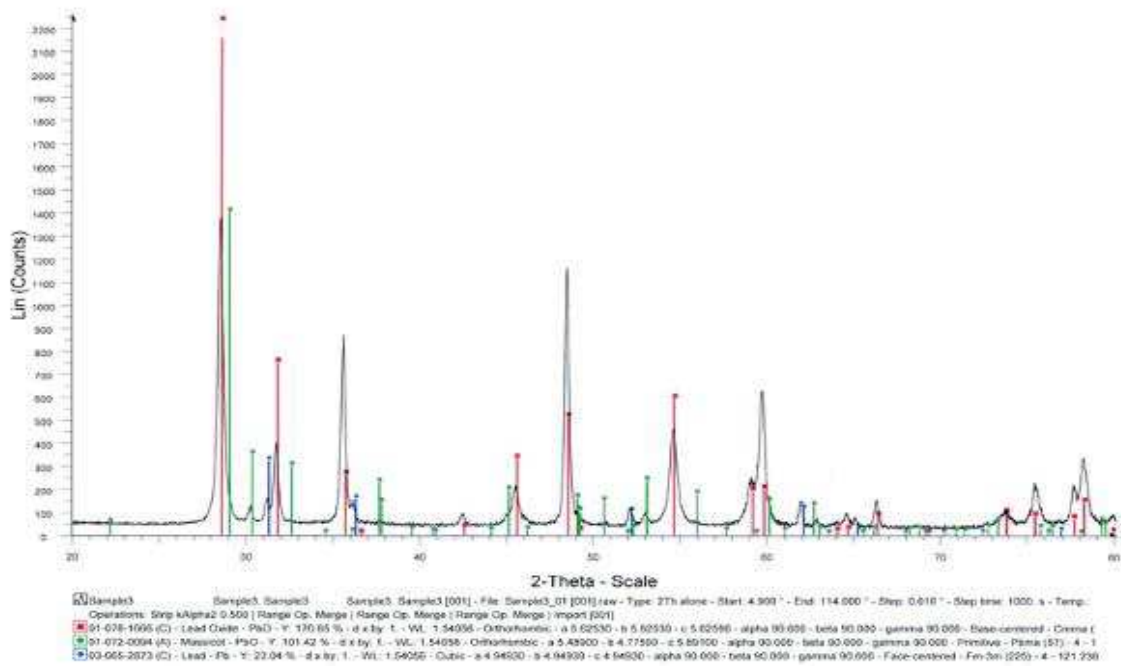
Figure 23: Diffractogram of the Barton pot lead oxide used for preparation of NAM paste.
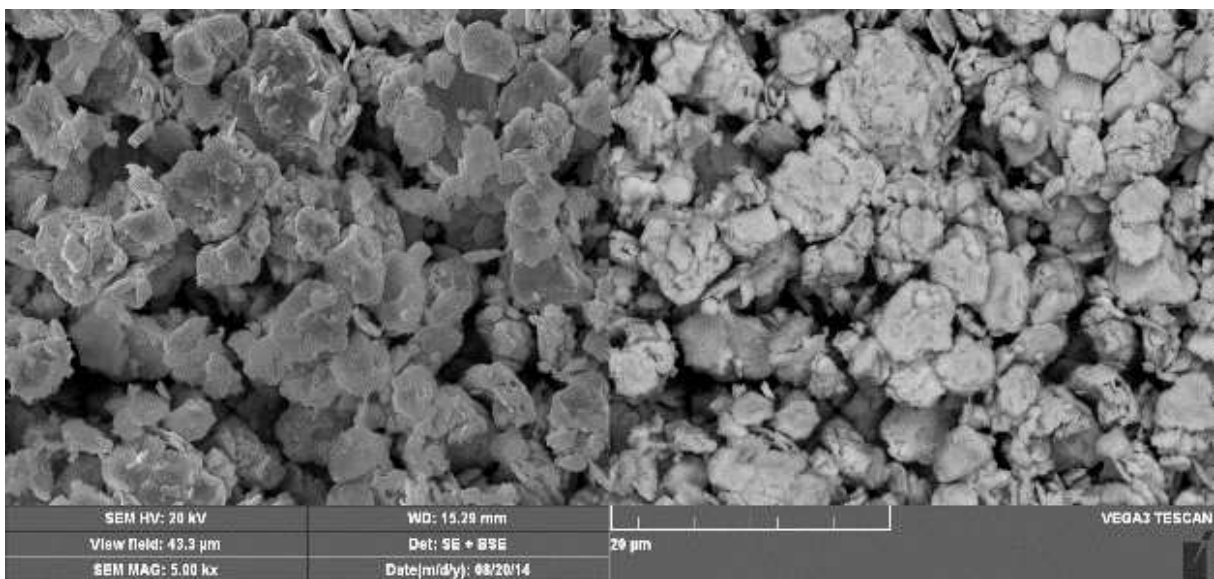
Figure 24: Morphology of the Barton pot leady oxide used in NAM paste.

We prepared the paste by hand and automated mixing of its components using corundum pestle, mortar, and automated mixer EL1 (Eirich, Germany). We deposited the paste on negative grids (Figure 25a) to form negative electrodes (Figure 25b).

A specialized mixer was purchased (EL1 Eirich, Germany) for the fabrication of the NAM paste, and then modified to create a vacuum mixer which could provide the constant temperature of ~42ºC under vacuum (at the residual pressure of 80 mbar). The vacuum mode of the mixer now allows for precise temperature control of the NAM paste during the addition of sulfuric acid which then allow for control of the structure and particle size of the NAM (tribasic lead sulfate $3PbO \cdot PbSO_4 \cdot H_2O$ (3BC) at T>50ºC) which is required for transportation applications at HRPSoC. It is critical to control the mixture's temperature of the mixture as adding sulfuric acid to the water-based paste causes uncontrollable self-heating. The paste density of 4.0-4.2g/cm^3 was controlled for each NE. The NAM paste was coated on lead grids by a doctor blade with the subsequent compression in the hydraulic press at a pressure of 10 Kg/cm^2.

The modified vacuum mixer EL-1 provides the reproducible quality of LAB electrode's pastes due to uniform mixing of all components, continuous control of temperature, and paste density. The paste density is proportional to the measured increased electric power required to support the same speed due to the continued paste solidification. The working conditions of the vacuum mixer EL-1 at the NAM paste fabrication are as follows:

- the rotation speed of the tilted chamber (20º) is 20-30 rpm
- the rotation speed of the rotator - 280 rpm (for dry mixture) and 30 rpm (for a wet paste)
- residual pressure under vacuum conditions: 80 mbar and T~42ºC
- spray of sulfuric acid
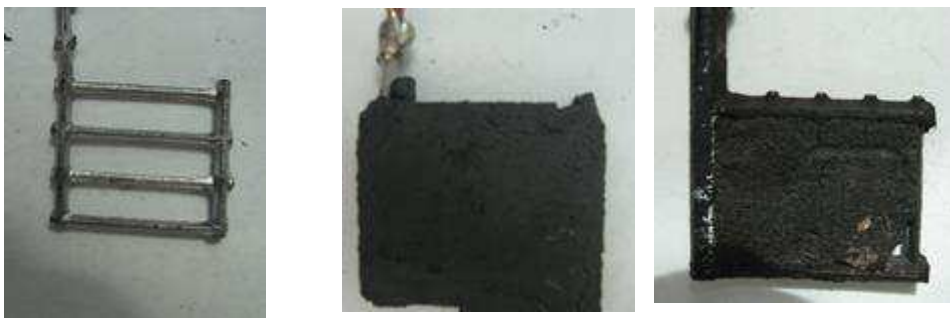
a)   b)   c)

Figure 25: Components of lead-acid battery and asymmetric supercapacitors: a) negative lead grid, b) graded negative electrode, c) positive electrode

Curing of prepared NE was done in the automated humidity/temperature control chamber (ESPEC, Japan) (Figure .26b) at three stages:[69]

- Relative humidity (RH) 95%, 45ºC, 2h
- Relative humidity (RH) 60%, 50ºC,12h

- Drying – RH <1%, 60ºC, 12h

Soaking NEs took place by dipping them in sulfuric acid ($1.28 g/cm^3$) for 1h at 25ºC. The formation of synthesized NAMs and PAMs lead to the reduction of PbO to Pb and oxidation of Pb^{2+} to Pb^{4+}. The formation (charging) of the NEs was implemented using a multi-step program on a Solartron potentiostat. The profile utilized the following steps: 0.2 mA/cm² for 1h, 0.6 mA/cm² - 1h, 3mA/cm² - 1h, 6 mA/cm² - 12h, 9 mA/cm² - 20h. The charging process was stopped when the final voltage reached a stable value of 2.58V for 4-5 hours, corresponding to the fully charged voltage of a LAB.

The formation of LAB electrodes was carried out using multichannel potentiostat Solartron (Model 1480). To activate dry electrodes, we applied the galvanostatic polarization at 0.015A (current 5% of C20 for 1h) in the electrolyte H_2SO_4 (sg 1.28 g/cm³).

a)   b)

Figure 26: a) Mixer EL1 (Eirich, Germany) modified in NRC with the vacuum mode for the preparation of LAB electrode's paste: 1 - vacuum chamber, 2 - reactor with V=100ml, 3 - thermocouple, 4 - water sprayer; b) Humidity/Temperature curing chamber (ESPEC, Japan).

4.3 Development of AGM LAB Design and Integration of Negative and Positive Electrodes in AGM LAB

The in-house fabricated AGM LAB test cell (2V) hardware consisted of a polypropylene case (1) and a PP insert (2). The design allowed for the compression of the electrode assembly between the two walls of the cell by screwing in four PVC bolts (3) (Figure 27) at the quantitative control of an applied torque for every bolt using a dynamometric screwdriver to achieve the reduction of the separator thickness by 20%.[70] Bolts push the insert in the direction of the applied load. The described test cell on Figure 27 was used for the development of a HB prototype and characterization of the baseline AGM LAB (2) and AGM HB (2V). An additional jig was developed and fabricated for the quantitative control of an electrode assembly compression in the LAB test cell (Figure 28) at the pressing a side insert by a pusher of the jig with the visual control of the AGM compression using narrow paper rulers on cell corners.

An AGM lead acid battery test cell (2V) was assembled by combining one negative electrode (2.2 cm x 2.2 cm) between two positive electrodes (2 cm x 2 cm), with their separation controlled by the AGM. The PE electrode's current collectors were soldered together with the Pb wire (3mm diameter) using a 100W soldering iron. The AGM separator was oversized compared to the LAB electrodes to reduce side currents. Finally, the AGM was soaked together with the electrodes in electrolyte during the activation stage of LAB.
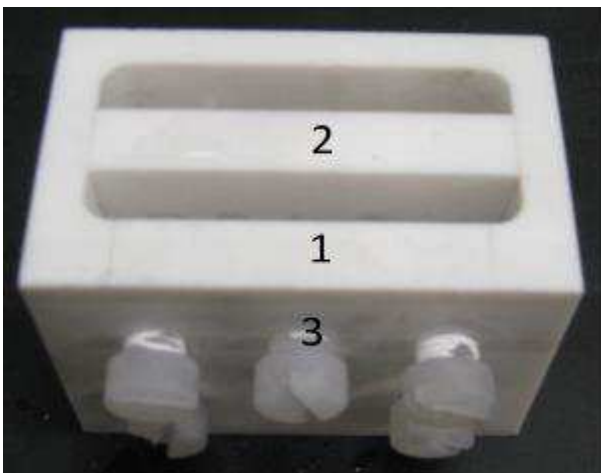
Figure 27: AGM LAB hardware: 1- polypropylene case, 2- movable insert, and 3-PVC bolts.

Figure 28: Jig for the quantitative control of an electrode cell compression: 1- base, 2-blocker, 3- pusher, and 4- digital controller of work loading.

4.4 Electrochemical Test of AGM LAB

All fabricated negative electrodes with different carbon type (KB 600J, YP80, AB50) and design (one or two layers) were tested in the baseline AGM LAB cell (2V). The electrochemical characterization of the most promising negative electrodes and commercial (Surrette Battery Co.) baseline negative electrodes for comparative evaluation of developed NE included two basic tests:

- A capacity test and rate map at four charge/discharge rates (1C, 0.5C, 20.2C, 0.1C) at the 100% DoD at cell voltage 1.7V (fully discharged battery) -2.45V (fully charged battery). The capacity of a small baseline AGM LAB (2V) and HB 73 were rated mainly at 1C discharge rate at 100% SoC. The galvanostatic mode was used for the capacity test.
- A cycle test for the estimation of the cycle life including the accelerated test (10-100 cycles) at 50% SOC in the cell under voltage range 2-2.45V. This test is based on a galvanic cycling method of the measurement of a cell voltage response under the constant current. A Galvanic cycling procedure was used for the cycle test.

The cyclability test was conducted at the high rate of 0.5C and 50% SoC in a cell voltage window of 2-2.45V.

Galvanostatic and galvanic cycling procedures were applied to NE as a working electrode with negative polarity for evaluation of the battery cycle life and capacity. The actual discharge capacity of the baseline AGM LAB with the commercial NE at different C rates (1C, 0.5C, 0.1C, 0.1C) at 100% SoC (12.45-1.75V) are shown in Figure 29.

The rated discharged capacity of AGM LAB and AGM HB was estimated at a rate of 1C after reaching 100% discharged battery at a resulting voltage cell of 1.7V.[69] The baseline AGM LAB cell contained the commercial standard negative electrode (2.2 cm x 2.2 cm) and 20%

compression of the AGM separator impregnated with the sulfuric acid electrolyte (1.28 g/cm^3).
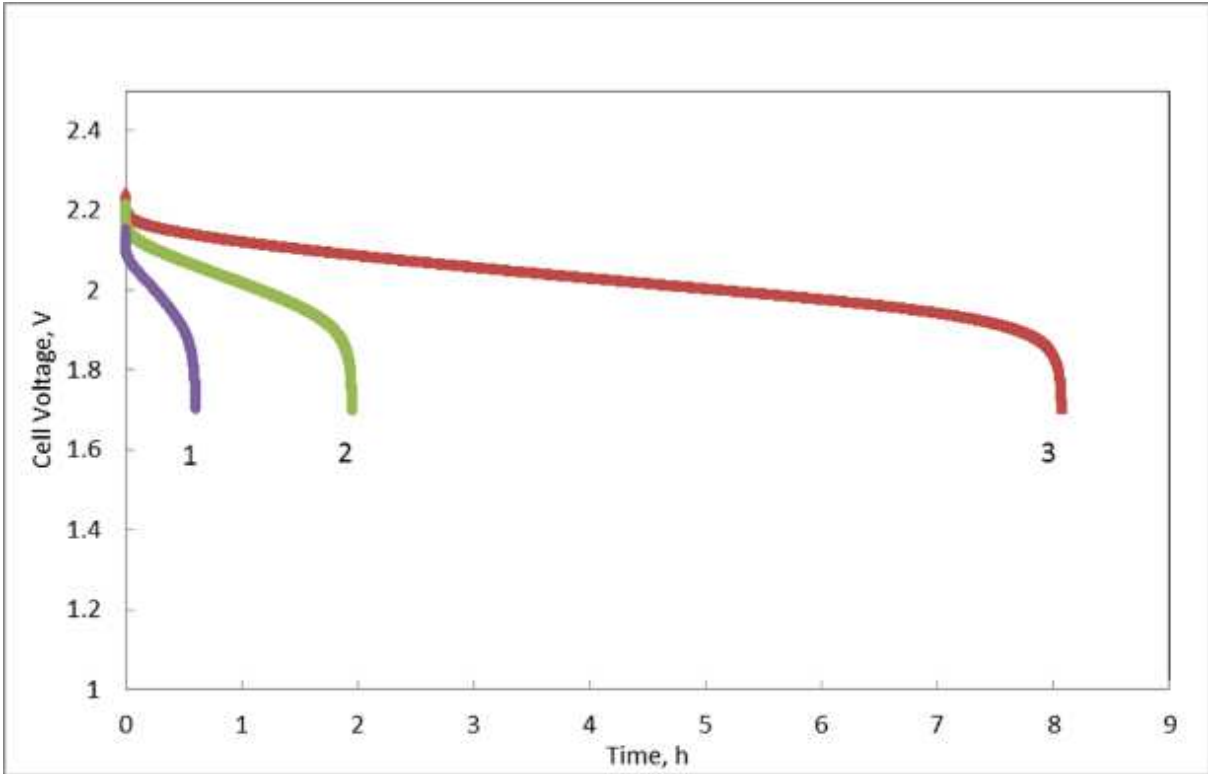
Figure 29: Lead acid battery (2V) discharge capacity curve at different discharge C-rates: 1-1C, 2 - 0.2C, 3- 0.5C.

The discharge rates are given in C-rate, which means that 1-Ah-battery would discharge/charge at 1A. The actual measured discharge duration of 0.75h at 1C discharge rate for the small baseline AGM LAB with a nominal capacity of 0.25Ah, shows less than 100% capacity. This is normal for most lead-acid battery technologies, where a reduction in capacity for increasing of C-rates is often seen vs their rated capacity which is often measured at the 20h-discharge rate[69,71]. This reduction is described by Peukert's law (Figure 29). Peukert discovered the reduction of the rated capacity at the faster discharge in our case from 0.05C (rated capacity for LAB) to 1C. However, small LABs could be rated at a 1C discharge rate. The actual capacity of the baseline AGM LAB (2V) 0.75 Ah is close to its nominal capacity of 1Ah at 1C rate (Table 12).

The cycling test of the baseline LAB with the commercial NE (0.15%C) was conducted at the high charge/discharge rate of 0.5C, 50% SoC (2-2.45V). The typical HRPSoC test for HEVs/EVs is not optimal for battery-electric locomotives. The baseline AGM LAB demonstrates the limited discharge capacity of 0.04 Ah after twenty cycle tests (Figure 35, Capacity curve 1).

Table 12: Actual capacity of the baseline AGM LAB with the commercial negative electrode at different C-rates

Discharge capacity, h / C rate	1C	0.5C	0.2C
Nominal capacity, h	1	2	5
Actual capacity, h	0.75	2	8

A detailed analysis of optimal carbon content for LAB's negative electrodes in order to reduce the accumulation of the non-conductive lead sulfate on their surface has been conducted.[58-65] The carbon mesoporous acetylene black (AB50) with the specific surface area $75m^2/g$ has been selected as the main type of carbon for NE in this work. A limited addition of a conductive carbon additive, i.e. carbon black C45, typical for supercapacitor electrodes (section 2.3), increases the effect of the mixed carbon additive as the expander for NEs. In this work we used the carbon-based mixture AB50:C45=8:1.

Several alternative carbon additives, such as the carbon black YP-80 and KB-600J (TKK) have been tested. These additives have higher specific surface areas and lower parts of meso- and macrospores compared to carbon AB50 which limits diffusion of the electrolyte into NE. NEs with higher carbon concentration (1-2%) compared to conventional LAB NEs with 0.1-0.2wt% C have the higher conductivity and lead utilization.

NEs with 0.7wt% C (AB50:C45=8:1) and two layers with 1.2%C and 0.7wt% C (C-(AB50:C45=8:1) were fabricated and tested. Cycle test results of one such negative electrode with optimal carbon concentration of 0.7 wt % C (AB50:C45=8:1) is presented in Figure 30.

AGM LAB with GNE demonstrated at least more than twice higher capacity compared to the baseline AGM LAB at the high charge/discharge currents during 20 cycles (Fig.30, Capacity Curve 3). This performance improvement was due to the reduced sulfation of NEs at their high carbon content and an optimal carbon distribution strengthening the GNE structure. However, according to the state-of-the-art (SOTA)[66,67,69], there is a carbon concentration limit (2wt.%) in NEs that causes loss of the mechanical integrity of NAM and the necessary addition of low conductive polymer fibers for NAM strengthening. A range of carbon concentrations of 0.3-1.2wt% in NEs was selected in Figure 30. The cycle test of AGM LAB at 0.5C, 50% SoC (2-2.45V) with different compositions of negative electrodes was conducted: 1) commercial negative electrode with 0.15%C (baseline AGM LAB), 2) NE with 0.7wt%C (AB50:C45=8:1), and 3) graded NE with two layers containing 1.2 and 0.7 wt% C (AB50:C45=8:1).
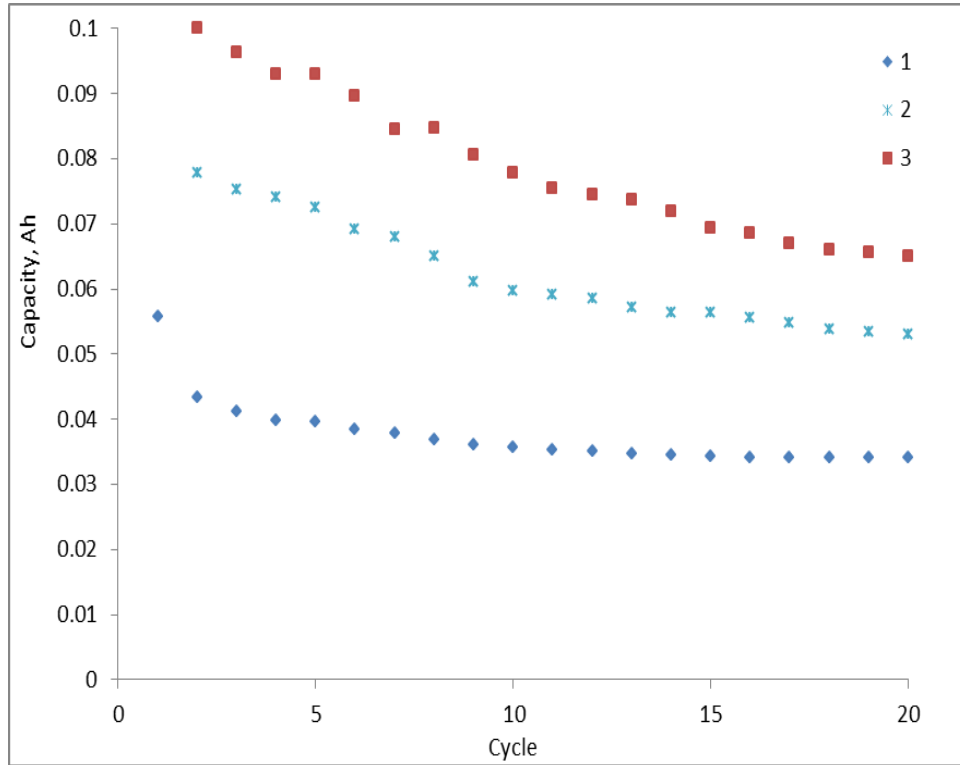
Figure 30: Cycle test of AGM LAB at 0.5C, 50% SoC (2-2.45V) with different composition of negative electrodes: 1) commercial negative electrode with 0.15%C (baseline AGM LAB), 2) NE with 0.7wt%C (AB50:C45=8:1), 3) graded NE with two layers containing 1.2 and 0.7wt%C (AB50:C45=8:1).

5 DEVELOPMENT OF A HYBRID BATTERY

5.1 Integration of AGM LAB and Asymmetric Supercapacitor in a Hybrid Battery

The developed and fabricated advanced electrodes for the asymmetric supercapacitor and advanced AGM LABs with high carbon content, and their distribution in the electrode coating, were assembled in the three-electrode HB (two positive and one negative electrodes) at 20% compression of the AGM separator.

5.1.1 Design of Hybrid Battery Hardware

The hybrid AGM LAB cell prototype with the graded negative electrode compressed with the carbon ASC electrode isolated by an AGM separator from the two positive formed electrodes (Surrette Battery Co.) was prepared according to the modified method.[70] The hybrid sealed AGM LAB cell prototype was pressed to achieve AGM compression by 20% for the improvement of the battery efficiency (Figure 31). The Teflon cell (1) has one graded electrode (3) compressed with the ASC's carbon electrode (4) (thickness 1200µm, 80% YP-80F +10% C45+5% PTFE+5% PbO), AGM (2), and two commercial LAB positive electrodes (5) (Figure 31a). The assembled cell was compressed using four PVC bolts (6) (Figure.31a).

5.1.2 Design of the Hybrid Battery Cell Configuration (Design of Negative Electrode)

Taking into account the development of NE for hybrid batteries to reduce their sulfation during the battery operation, a new graded negative electrode (GNE) was developed and fabricated. The GNE consists of two layers (the first layer contains 1.2 wt%C and the second layer - 0.7wt.%C) on the negative lead grid with a ratio of the conductive carbon black C45 and acetylene carbon black AB50 (AB50:C45=8:1) with the specific surface area of $75m^2/g$ (Table 13).

Table 13: Design of the graded negative electrode (GNE) for a hybrid battery

Hybrid negative electrode		
Graded negative electrode		ASC electrode
1st layer	2nd layer	ASC
1st Layer of LAB NE with high carbon content (1.2%) (battery electrode side)	2nd Layer of LAB NE with low carbon content (0.7%) (ASC electrode side)	ASC carbon electrode (80% YP80 +10% C45 + 5%PbO + 5% PTFE).

The acetylene carbon black AB50 was selected for NE according to the detailed Boden's study of the optimal carbon material for LAB's NEs.[65] The effective conductive carbon black C45 was selected due to its positive tests as a conductive additive in ASC carbon electrodes.

The concentration of carbon gradually decreases when moving from the battery-like surface of the hybrid NE to its interface with the developed ASC's carbon electrode (80wt% YP-80 [activated carbon] +10% C45 [conductive additive] + 5% PTFE+5% PbO_2) (see section 2.1 of this report). The negative ASC carbon electrode will respond quickly to a high rate charge/discharge by accumulating energy in a double layer. Thus, the graded negative electrode exhibits properties of both a capacitor and a battery electrode.
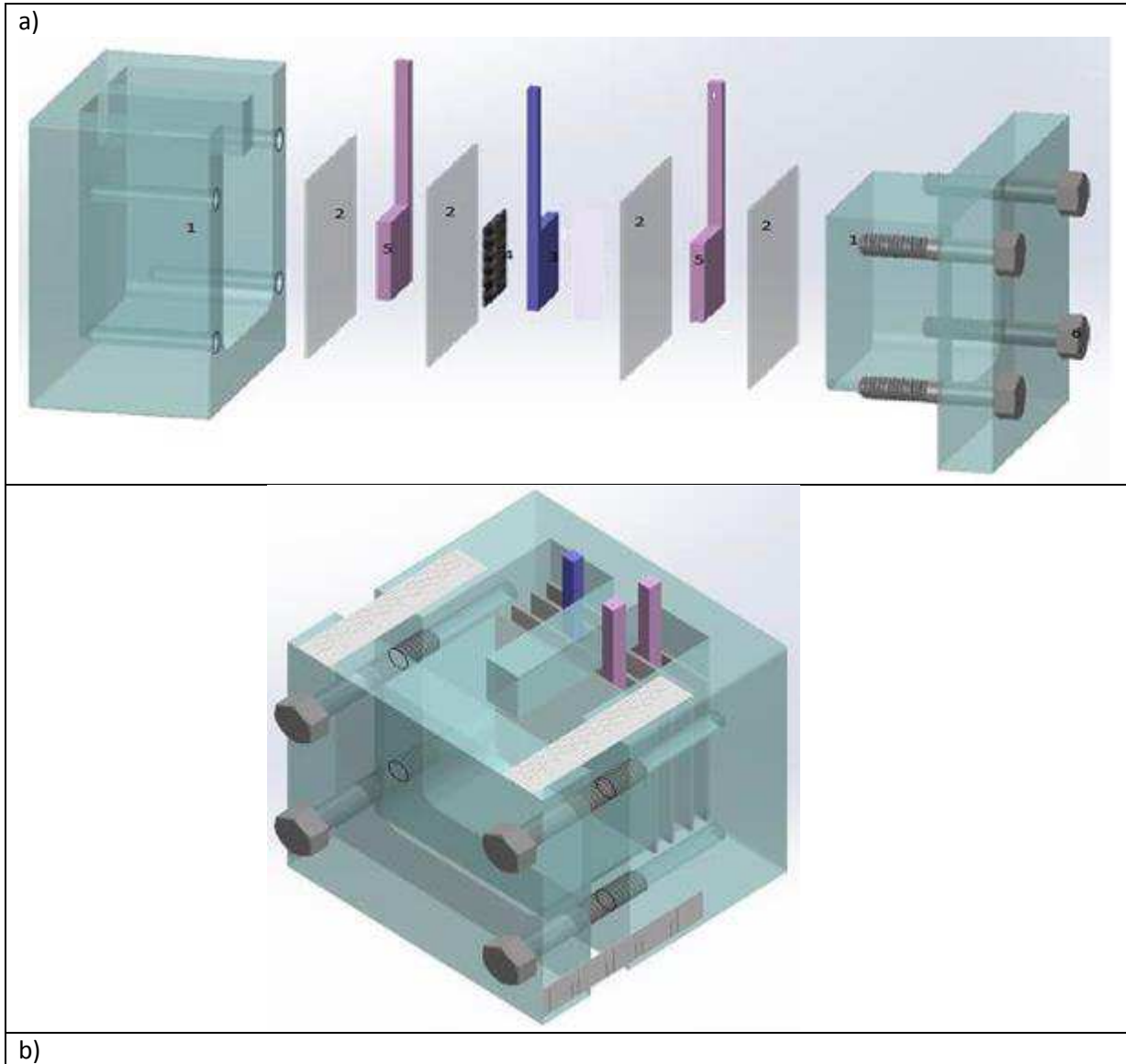
Figure 31: Design of hybrid battery cell (2V) prototype: a) disassembled HB (2) with components as follows:1-Teflon case, 2-AGM separators, 3- negative electrode, 4-ASC negative electrode, 5- positive electrode, 6- Cover with PVC bolts; b) assembled HB (2V).

The sulfation of GNE will be eliminated on its ASC side, and a gate for HSO^{4-} migration will not be blocked during heavy cycling. The charge transfer will be remarkably improved, and

eventually the battery cycle life will be extended. This configuration of a graded negative electrode of the hybrid battery has not been claimed in the relevant patent literature, namely the comprehensive Lam's patent.[55] Lam and co-inventors in their comprehensive patent have disclosed a variety of combinations in which negative and positive electrodes of Pb-acid batteries and asymmetric supercapacitors may be combined to form a hybrid energy storage device.[55] According to Lam et al., suppression of hydrogen gassing can be achieved by the use of additives (preferably lead oxide) to the capacitor negative electrodes. The concept of a hybrid battery can be realized for both a flooded-electrode design and a sealed valve regulated LAC design.

5.2 Electrochemical Test of the Developed Hybrid Battery

Based on the beneficial performance of the developed graded negative electrode (GNE), two layers containing 1.2%C and 0.7%C (AB50:C45=8:1) in AGM LABs (Table 13) were assembled in the hybrid battery (Figure 31) and tested. The main part of this HB is a sealed AGM LAB with 20% compression of AGM separator.

The advantage of GNE is in its strong mechanical strength at a high content of carbon, increasing conductivity, specific surface area, and porosity. A separate ASC carbon electrode is attached to the GNE's layer with lower carbon content. The cycle test results of the hybrid batteries with three different NEs are presented in Figure 32. This shows that HB with GNE (Figure 32, Curve 1) containing higher total carbon content (AB50:C45), specifically in its first layer (facing the battery side), exhibits the higher capacity at the enhanced discharge C-rate - 0.5C than that of HB with other GDE with less total carbon content (Curve 2) and HB with NE with high carbon content of 0.7% (Curve 3). The cycle tests were conducted after activation of dried electrodes in galvanostatic mode (0.015A, for 24h) according to the Surrette Battery's protocol.

The best stable capacity achieved so far (0.1Ah) by GNE containing high carbon loading (CB50:C45=8:1;1st Layer-1.2%C+ 2st Layer -0.7%C) exceeds almost twice the capacity of the baseline AGM LAB (Figure 30, Curve 1), including commercial NE with low carbon loading of 0.15%.This result is interpreted in terms of lower sulfation of HB GNE due to high carbon loading that causes the formation of a more stable electrode matrix structure than that of conventional LAB with commercial NE. The size of lead sulfates particles on the surface of GNE after the cycle test at high currents is lower than that on the surface of a commercial electrode.

49
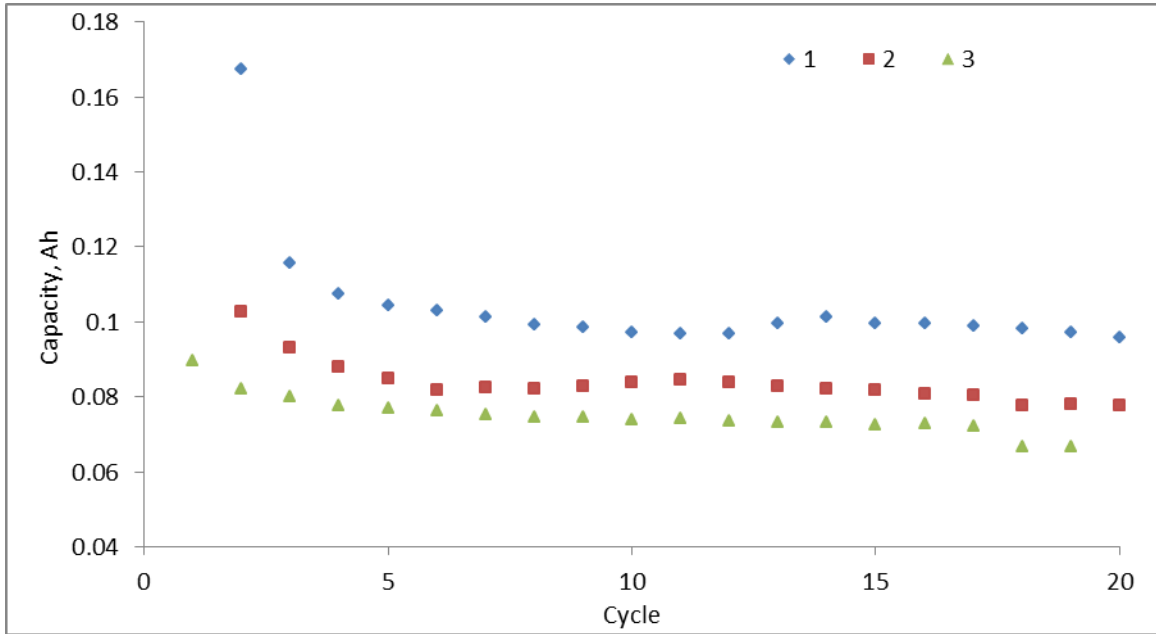
Figure 32: Baseline capacity test of hybrid battery at 0.5C and 50%SoC (2-2.45V) with negative electrodes (NE) with high carbon (AB50:C45=8:1) content: 1- graded NE 1st Layer-1.2%C+ 2st Layer -0.7%C, 2-graded NE-1st Layer-0.7%C+ 2st Layer – 0.3%C, and 3- 0.7%C.

5.3 Fabrication of Hybrid Battery Cell Prototype

A method for assembling a hybrid battery cell prototype consists of next stages.

One negative and two positive electrodes were cut from commercial electrodes supplied by Surrette. The active surface area was about 22 x 22mm for both positive and negative electrodes.

Carbon electrode was prepared from YP-80F activated carbon (Kuraray), Super C45 conducting carbon (Timcal), and PTFE dispersion solution (Sigma-Aldrich). Chemicals were weighed into a beaker, and then dispersed in ethanol at its boiling temperature. A jelly paste was formed when most of the ethanol evaporated. The paste was then repeatedly pressed and rolled to form a free standing sheet and then rolled into a 1mm thick sheet. Then the formed sheet was placed into the vacuum oven to dry at 120ºC overnight. Two carbon electrodes of the same dimensions as positive and negative electrodes were cut and weighted. These two carbon electrodes were vacuumed and impregnated with sulfuric acid solution.

Four pieces of AGM separator of 50 mm x 50 mm were prepared. The thickness of all carbon, positive, and negative electrodes was measured for the cell assembly reference.

To assemble a hybrid lead-acid battery, two carbon electrodes were placed on each side and opposite to negative electrode, two AGM sheets were then placed on each side, the two positive electrodes and two AGM sheets on the most outward. These materials were then put

into the PTFE test cell (Figure 31). PVC screws were used to press the electrode assembly and to reduce the AGM thickness by 20%. To control the clamping thickness, we used ruler strips at four corners of the cell to ensure it was evenly clamped and fit the cell gap.

The whole HB cell assembly was then placed into a plastic zip bag. Electrode tabs penetrated through the plastic bag for easy wire connection. Then the bag was sealed with a beeswax/rosin mixture to avoid acid penetration into the electrode tabs.

Sulfuric acid (1.28 g/cm^3) was added into the plastic zip bag for electrode soaking within 1 hour. The excess of acid was then removed during sealing of the plastic bag.

6 CONCLUSIONS AND RECOMMENDATIONS

Conclusions

The developed a cost-effective hybrid battery (2V) lab-prototype with graded negative electrodes demonstrates more than twice the capacity and a longer cycle life than conventional lead-acid batteries at high charge/discharge rates. Capitalization on the achieved technical targets and core-capabilities for the fabrication of HB electrodes and the battery prototypes is expected to provide a significant improvement of cycle life and cost-efficiency compared to the performance level achieved

Recommendations

Continuation of this project with further support from Transport Canada would allow for the movement of the HB battery development to the next stage, namely the design and fabrication of more powerful HB (12V) batteries for use in battery-electric locomotives (BEL).

Accomplishments

In conclusion, based on the work done, the following main tasks were completed:

1. The design, development, and fabrication of a cost-effective hybrid battery (2V) lab-prototype with graded negative electrodes (GNE) was completed. It was shown to have more than twice the capacity and a longer cycle life than conventional lead acid batteries at high charge/discharge rates.

2. The design and fabrication of a graded negative electrode was completed, which had both a high carbon loading (1.2wt%, (AB50:C45=8:1) on the battery surface layer, and low content (0.7wt.%) on the ASC side. This graded negative electrode was more durable than negative electrodes of conventional lead acid batteries.

3. An advanced ASC carbon electrode (80wt%C(YP-80)+10%C(C45) 5%PTFE+5%PbO_2) for HBs was developed and produced that showed high durability, conductivity, and capacitance for HBs.

REFERENCES

1. Environment and Climate Change Canada, Reducing Canada's greenhouse gas emissions, https://www.ec.gc.ca/dd-sd/default.asp?lang=En&n...1, February 15, 2013. Accessed on February, 2016.

2. Simon P., Gogotsi Y., Capacitive Energy Storage in Nanostructured Carbon–Electrolyte Systems, *Accounts of Chemical Research* 46, 2013, 1094-1098

3. Miller J., Burke A.F. Electrochemical capacitors: Challenges and opportunities for real world applications. *Electrochem. Soc. Interface* 17, 2008, 53–57.

4. Weighall M., *Supercap ups or downs*, Batteries + Energy – Storage Technology*, BestMag,* 22, Autumn 2008, 79 – 86.

5 Simon P., Gogotsi Y. Materials for electrochemical capacitors, *Nature Materials* 2008, 7, 845-54.

6 Jayalakshmi M., Balasubramanian K. Simple Capacitors to Supercapacitors - An Overview, *Int. Journal of Electrochemical Science* 3, 2008, 1196-1217.

7 Miller J.R., Simon P*.,* Electrochemical Capacitors for Energy Management *Science* 321, 2008 651-652.

8. Burke A.J*.,* Ultracapacitors: Why, how, and where is the technology, J of *Power Sources,* 91, 2009 37-50.

9. Simon P., Burke A., Nanostructured carbons: double-layer capacitance and more, *The Electrochemical Society Interface*, Spring, 2008, 38-43,

10. Naoi K., Simon P., New materials and new configurations for advanced electrochemical capacitors, *The Electrochemical Society Interface*, Spring, 2008, 34-37.

11. Pandolfo, A.G.; Hollenkamp, A.F., Carbon properties and their role in supercapacitors, *Journal of Power Sources* 157, 2006, 11-27.

12. Zhai Y., Dou Y., Zhao D., Fulvio P.F., Mayes R.T., Dai,S. Carbon materials for chemical capacitive energy storage. *Adv. Mater*. 23, 2011, 4828–4850.

13. Conway B.E., Electrochemical Supercapacitors, *Kluwer Academic/Plenum Press*, New York, 1999.

14. Wu M.S., Chiang P.C.*,* Fabrication of Nanostructured Manganese Oxide Electrodes for Electrochemical Capacitors, *Solid-State Lett.,*7, 2004, A123

15. Sugimoto W., Iwata H.Y., Murakami and Y. Takasu, Electrochemical Capacitor Behavior of Layered Ruthenic Acid Hydrate *J. Electrochem. Soc.*, 2004,151, A1181

16. Dong X., Shen W., Gu, L., Xiong Z., Zhu Y., Li H., Shi J.*,* MnO_2-Embedded-in-Mesoporous-Carbon-Wall Structure for Use as Electrochemical Capacitors, *J. Phys. Chem*. B, 2006, 110, 6015

17. Zhang Y., Feng H., Wu X., Wang L., Zhang A., Xia T., Dong H, Li X., Zhang L., Progress of electrochemical capacitor electrode materials: a review. *Int. J. Hydrogen Energy*, 2009, 4889-4899

18. Conway B.E., Birss V., Wojtowicz J*.,* The role and utilization of pseudocapacitance for energy storage *J. Power Sources*, 66,1997, 1-5

19. Chuang S.M., Huang C.W., Teng H, Ting J.M., Effects of carbon nanotube grafting on the performance of electric double layer capacitors,*Energy and Fuels,* 24, 2010,6476

20. Katz, H.E., Searson, P.C., Poehler, T.O. Batteries and charge storage devices based on electronically conducting polymers, *J. of Materials Researc*h 25,2010, 1561-1574.

21. Snook, G.A., Kao, P., Best, A.S., Conducting-polymer-based supercapacitor devices and electrodes *J. of Power Sources* 196,2011, 1-12.
22. Oyaizu K., Nishide H., Radical Polymers for Organic Electronic Devices: A Radical Departure from Conjugated Polymers *Advanced Materials* 21, 2009, 2339-2344.

23. Suga T., Ohshiro H., Sugita S., Oyaizu K., Nishide H., Emerging N-Type Redox-Active Radical Polymer for a Totally Organic Polymer-Based Rechargeable Battery, *Advanced Materials* 21,2009,1627-1630.
24. Nakahara K., Iriyama J., Iwasa S., Suguro M., Satoh M., Cairns E., Al-laminated film packaged organic radical cathodes for Li rechargeable batteries, *J. Power Sources* 163, (2007),1110-1113.

25. Burke A., Ultracapacitors: Why, How, and Where is the Technology, *J. Power Sources*, 91, 2009, 37

26. Kisacikoglu M., Uzunoglu M., Alam M., Load sharing using fuzzy logic control in a fuel cell/ultracapacitor hybrid vehicle *Int. J. Hydrogen Energy*, 2009, 34, 1497-1507

27. Ma K., Nam W., Yoon, Yang X., Ahn K., Oh K, Kim K., A novel concept of hybrid capacitor based on manganese oxide materials, *Electrochem. Commun.,* 9, 2007, 2807-2815

28. Laforgue A., Simon P., Fauvarque J. F., Sarrau J. F., Lailler P*.,* Stable Graphene-Polyoxometalate Nanomaterials for Application in Hybrid Supercapacitors. *J. Electrochemical Soc.* 148, (10), 2001, A1130-A1134.

29. EGY068B - Supercapacitors: Technology Developments and Global Markets, *BCC Research*, 2015

30. Electrochemical Double Layer Capacitors: *Supercapacitors 2015-2025*. IDTechEx, 2016

31. Chmiola J., Largeot C., Taberna P.L., Simon P., Gogotsi Y*.,* Desolvation of Ions in Subnanometer Pores and Its Effect on Capacitance and Double-Layer Theory*, Angewandte Chemie* 120, 2008,3440-3443.

32. Lin R., Taberna P.L., Chmiola J., Guay D., Gogotsi Y., Simon P., Microelectrode Study of Pore Size, Ion Size, and Solvent Effects on the Charge/Discharge Behavior of Microporous Carbons for Electrical Double-Layer Capacitors, *J. Electrochem. Society,* 156, 2009, A7-A12.

33. *Frost & Sullivan* Report NDBC-27; February 2015.

34. Miller J. R., Burke A. F., Electrochemical capacitors: challenges and opportunities for real-world applications, *The Electrochemical Society Interface,* Spring, 2008, 1753-1757.

35. Miller J. R., in *BESTMag Autumn*, 2010, 121-128.

36. Burke A., Ultracapacitor technologies and application in hybrid and electric vehicles, *International Journal of Energy Research* 34, 2010, 133-151.

37. Advanced lead acid battery consortium (ALABC) website: http://www.alabc.org/publications/bipolar-designs/view. Accessed on March 1, 2014

38. Sonic website: http://www.sonnenschein.org/PDF%20files/Gel Handbook Part 1.pdf

Accessed on March 10, 2014

39. *Handbook for Stationary AGM-VRLA Batteries*. Website: http://www.elektrotec-berlin.de .Accessed on March 13, 2014

40. Lam, N.P. Haigh, Phyland C.G., Huynh T.D., Novel technique to ensure battery reliability in 42-V Power Nets for new-generation automobiles, *J. Power Sources*, 144,2005, 552–559

41. Lam L.T., Haigh N.P., Lim O.V., Lwin T., Phyland C.G., Vella D.G., ALABC Project TE-1, Influence of trace elements, plate-processing conditions, and electrolyte concentration on the performance of valve-regulated lead-acid batteries at high temperatures and under high-rate partial-state-of-charge operation, Final Report: August 2003–July 2005, CSIRO Energy Technology, Investigation Report ET/IR809R, July 2005, 43 pp.

42.Trinidad F., Valenciano J., Dyson I., Hollenkamp A.F., Ozgun H., *ALABC Project N4.2*, Optimization of the negative active material and PSoC cycle life of VRLA batteries for 42V mild hybrid applications, Final Report: July 2003–June 2005. Issued: September 2005, 117 pp

43. Osumi S., Shiomi M., Nakayama K., Sawai K., Funato T., Watanabe M., Wada H., *ALABC Project N5.2,* Development of additives in negative active material to suppress sulfation during high-rate-partial-state of charge operation, Final Report: July 2003–June 2005, Issued: May 2005, 51 pp.

44 Lam L.T., Nigei Haigh, Christopher Phyland, David Rano, High performance energy storage devices, US patent 2007/0104981 A1, 2003

45. Website of Axion Power International Inc.: www.axion.com

46. Website of Xtreme Power: www.xpcc.com

47. Varakin I.N, Klementov A.D., Litvienko S.V., Starodubtsev S.V., Stepanov A.B., Application of ultracapacitors as traction energy sources. Proceedings of the Seventh International Seminar on Double-Layer Capacitors and Similar Energy-Storage Devices, Deerfield Beach, FL, USA, 8–10 December, 1997

48. Razoumov S., Klementov A., Litvinenko S , Belyakov A. Asymmetric electrochemical capacitor and method of making, US Patent 6,222,723 B1, 2001.

49. Buiel E.R, Eshkenazi V, Rabinovich L., Sun W., Vichnyakov V., Swiecki A.J., Cole J.E. Negative Electrode for Hybrid Energy Storage Device , US Patent 20110281162, 2011

50. Buiel R.B. Cole J.E. Electrode with reduced resistance grid and hybrid energy storage device having same US Patent, 8202653, 2012

51. Axion Power – A Battery Manufacturer Charging Forward http://www.altenergystocks.com/archives/energy_storage/batteries/November, 18, 2012. Assesed February 11, 2014

52 Axion picks up another patent for its lead-acid battery-supercapacitor hybrid cell, Website www.greencongress.com, Assesed February 11, 2014

53.Schoenung S., Storage system cost update, Study for the DOE Energy Storage Systems Program (Report SAND2011-2730). DOE Sandia National Laboratories website: www.sandia.gov.Assesed February 11, 2014

54. Konrad T., Axion Power's Potential For Explosive Growth, Forbes website: https://www.forbes.com/sites/tomkonrad/2013/07/23/axion-powers-potential-for-explosive-growth/#1573a0d64983. Accessed on February 12, 2014

55. Lam L.T., Nigel N.P., Phyland C.G, Rand D.A., High performance energy storage devices, U.S. Patent 7,923,151, 2011

56. Lam L.T., Louey R., Development of ultra-battery for hybrid-electric vehicle applications, *J. of Power Sources*, 158, 2006, 1140-1148

57. Ernos D.G., Hund T.H., Shane R., Report 11-3460 "Understanding and performance of carbon–enhanced lead-acid batteries," *Sandia National Laboratories*, 2014, 1, 1-17.

58 Shiomi M., Funato T., Nakamura K., Takahashi T.I,Tsubota M., Effects of Carbon in Negative Plates n Cycle-life Performance of Calve-regulated Lead/Acid Batteries, *J. of Power Sources*, 64, 1997, 147-152.

59. Ohmae T., Hayashi T., Inoue N., Development of 36-V Valve Regulated Lead-acid Battery. *J. of Power Sources*, 116 (2003), 105-109.

60. Spence M.A., Boden D.P., Wojcinski T.D., Identification of the Optimum Specification for Carbon to be Included in the Negative Active Material of a Valve-Regulated Battery in Order to Avoid Accumulation of Lead Sulfate During High-Rate Partial-State-of-Charge Operation.‖ *ALABC Research Project Designatio*n C1.1/2.1A, Progress Report 2, May 2008.

61 Spence M.A., Boden D.P., Wojcinski T.D., Identification of the Optimum Specification for Carbon to be Included in the Negative Active Material of a Valve-Regulated Battery in Order to Avoid Accumulation of Lead Sulfate During High-Rate Partial-State-of-Charge Operation.‖ *ALABC Research Project Designation* C1.1/2.1A, Progress Report 4, October 2009.

62 Calábek M., Micka K., Křivák P., Bača P., Bilko R., Lábus R., Significance Of Carbon Additive In Negative lead-Acid Battery Electrodes, *ALABC Project No. C 2.2, Final Report*, April 2008.

63. Micka K., Calábek M., Bača P., Křivák P., Lábus R., Bilko R., Studies of Doped Negative Valve-regulated Lead-acid Battery Electrodes, *J. of Power Sources*, 191 (2009), 154-158.

64. Calebek M, Micka K., Krivak P. Baca P., Significance of Carbon Additive in Negative Lead-acid Battery Electrodes. *J. of Power Sources*, 158 (2006), 864-867.

65. Valenciano J., Sanchez A., Trinidad F., Hollenkamp A.F., Graphite and Fiberglass Additives for Improving High-rate Partial-state-of-charge Cycle Life of Valve-regulated Lead-acid Batteries. *J. of Power Sources*, 158 (2006), 851-863.

66. Lam L.T.,Production and test of hybrid VRLA UltraBattery developed specially for high rate partial state-of-charge operation. ALABC project DP1.1. Final Report, 2007, ALABC website www. Accessed on February 19, 2014.

67. Lam L.T., Louey R., Development of ultra-battery for hybrid electric vehicles applications, *J. Power Sources*, 158, 2006,1140-1148.

68. White paper "UltraBattery$^{®}$: Benefits of a Breakthrough Storage Technology 2014, *Ecoult website*: www.ecoult.com. Accessed on May 10, 2016.

69. Pavlov D., Lead-acid Batteries. Science and technology, *Elsevier*, 2011, 631 p.

70. Pavlov D., Nikonov P., Lead-Carbon Electrode with Inhibitor of $PbSO_4$ Recrystallization in Lead-Acid Batteries Operating on HRPSoC Duty, *J. Power Sources*, 242, 2013, 380-399.

71. Jung J., Zhang L., Zhang J., Lead Acid Battery technologies, *CRC Press*, 2015, 350p.